Off Bragg Blazing For TM Polarization With Rectangular Gratings

by

Wei Chen

B. Eng. (Electrical Engineering) Zhejiang University, 1989

A THESIS SUBMITTED IN PARTIAL FULFILLMENT OF

THE REQUIREMENTS FOR THE DEGREE OF

MASTER OF APPLIED SCIENCE

in

THE FACULTY OF GRADUATE STUDIES

DEPARTMENT OF ELECTRICAL ENGINEERING

We accept this thesis as conforming

to the required standard

THE UNIVERSITY OF BRITISH COLUMBIA

Oct. 1994

Abstract

Perfect blazing to the m=-1 spectral order was once assumed to be possible for only Bragg angle incidence, i.e. for an angle$\theta_i = \sin^{-1}\left(\frac{\lambda}{2d}\right)$ from the normal to the grating surface, where d/λ is the grating period in wavelengths. The diffracted beam is then back in the direction of incidence, an inconvenience in most applications such as multiplexers, de-multiplexers and frequency scanned antennas. Off Bragg blazing is preferable and now can be done with high efficiency. Here off Bragg blazing for TM polarized incidence on rectangular groove gratings is investigated numerically and design curves are presented.

It is a consequence of reciprocity that off Bragg blaze angles must occur in pairs θ_1 and θ_2 and these are related by a generalization of the Bragg equation $\sin\theta_1 + \sin\theta_2 = \frac{\lambda}{d}$. For groove width to period ratios a/d=0.5 perfect off Bragg blazing occurs most frequently for periods 0.9<d/λ<1.0 and groove depth 0.1<h/λ<0.24. It is for periods d/λ in this range that the larger deviations $\theta_1 - \theta_2$ are possible. Off Bragg blazing is found to occur for 0.4<a/d<0.9999, but the larger deviations and hence the more potentially useful designs appear to occur for$a/d \approx 0.5$. The numerical results correlate well with earlier numerical and experimental data.

E.V.Jull

TABLE OF CONTENTS

LIST OF ILLUSTRATIONS

FIGURE

Acknowledgements

I am deeply grateful to my supervisor Dr. E.V.Jull for his advice and encouragement during the research, for his patient reading the original draft, for his valuable comments and correction of this thesis, and for the research assistantship I received from 1993 to 1994.

I would like to thank Dr. Dave Micheson for his patient help and constructive suggestion during the research, and especially for the computer program he offered for my use.

I would like to thank Mr. Al MacKenzie for his assistance in repairing the experimental instruments.

I would like to thank the Electrical Engineering Department in the University of British Columbia for the teaching assistantship I received in 1993.

Finally, I thank all friends in Canada for very wonderful two years of studying in Vancouver. Particularly, I am very grateful to my sister Polly Pu Chen, to whom I would like to dedicate this thesis. I would like to thank her and her family for all they did for me. Without her help I doubt if this thesis would have been completed.

Wei Chen

Chapter 1. Introduction

The problem of scattering by electromagnetic waves from a perfectly conducting grating with periodic surface was widely considered in the 1970's. To eliminate specular reflection from a conducting surface, blazed gratings were proposed to eliminate interfering specular reflection from metallic building surfaces such as airport hangers [12], as low-loss frequency multiplexers and as reflectors for frequency scanned antennas. Their wide potential use resulted in numerous published numerical studies as well as experimental results on the blazing property of diffraction gratings. A "blazed " grating is one in which the diffracted power is concentrated in a particular direction, in this case the direction of backscatter.

A plane electromagnetic wave incident on a perfectly conducting grating with periodic surface produces a scattered electromagnetic field, which is comprised of a finite number of homogeneous plane waves and an infinite number of evanescent waves.

The scattering angles θ_m, when expressed in terms of the grating period d, wavelength λ, and the angle of incidence θ_i from the surface normal, become:

$$\sin\theta_m = \sin\theta_i + \frac{m\lambda}{d} \tag{1.1}$$

This is called the grating formula in [1], where the mth diffracted order homogeneous plane wave will propagate away from the surface at angle θ_m if and only if $|\sin\theta_m| < 1$.Otherwise, if $|\sin\theta_m| > 1$,the mth diffracted order corresponds to an evanescent field which decays exponentially from the surface of the grating.

According to the grating formula (1.1), the dimensions of a grating can be carefully chosen so that the conducting surface will scatter only two spectral orders: the specularly reflected (m=0) which propagates at an angle θi, and the principal backscatter wave (m=-1) at an angle $\theta_{-1}$to the normal.

From equation (1.1), if the period d and wavelength λ satisfy the condition (1.2) only the specularly reflected order will propagate. Similarly, if inequality (1.3) is satisfied, the principal backscatter mode (m=-1) appears; if inequality (1.4) is satisfied, the second backscatter mode (m=-2) disappears; and if inequality (1.5) is satisfied, the principal forward scatter mode (m=1) disappears. So, if inequality (1.3, 1.4, 1.5) are satisfied simultaneously, only the m=0 and the m=-1 diffracted order will propagate as shown in Fig1.1 . Fig1.1 was first drawn by D.G.Michelson in his Ph.D. thesis

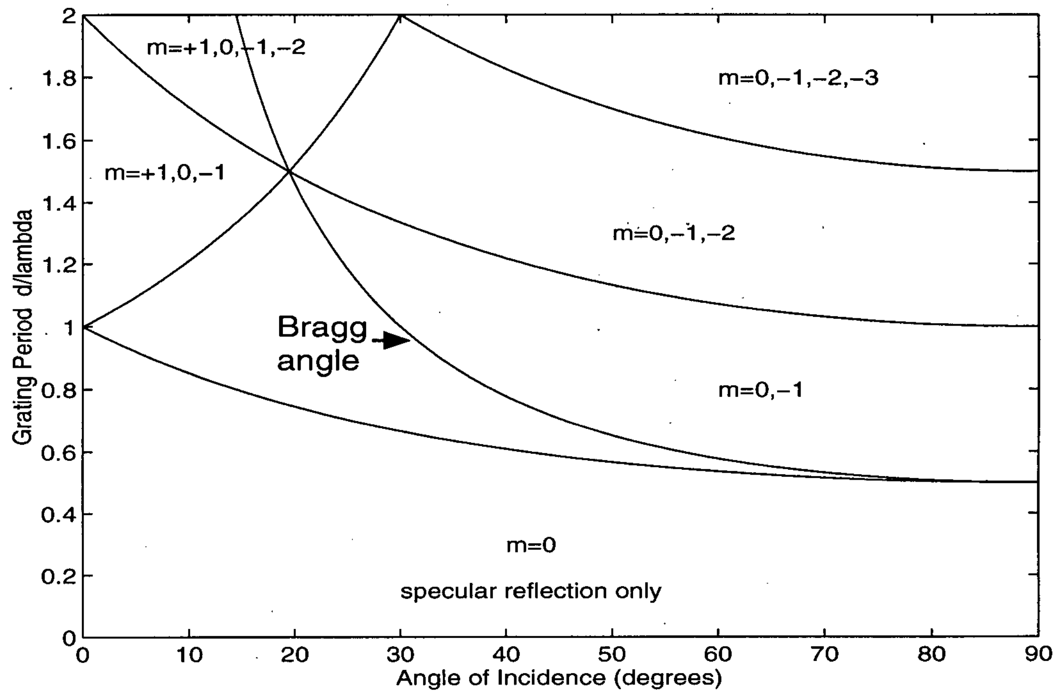

Figure 1.1: Propagating diffraction orders as a function of the grating period and the angle of incidence. From [8]

[8].

$$\sin\theta_i - \frac{\lambda}{d} < -1 \tag{1.2}$$

$$\sin\theta_i - \frac{\lambda}{d} > -1 \tag{1.3}$$

$$\sin\theta_i - \frac{2\lambda}{d} < -1 \tag{1.4}$$

$$\sin\theta_i + \frac{\lambda}{d} > 1 \tag{1.5}$$

For the Bragg angle condition, total power is converted into the principal backscatter mode (m=-1), and propagates back towards the source. So, using$\theta_{-1} = -\theta_i$and m=-1 into equation (1.1), we get the Bragg angle condition as (1.6) which is shown in Fig 1.1 also.

$$\sin \theta_i = \frac{\lambda}{2d} \tag{1.6}$$

Fig 1.1 also clearly illuminates the range where Bragg blazing occurs (i.e. $19.5^o < \theta_i < 90^o$,and $0.5 < \frac{d}{\lambda} < 1.5$).

Under the Bragg angle condition, we have a " nonreflecting" conducting surface, which was first investigated for TM polarization alone with the right-angle echelette grating profile. Then numerical studies of the blazing of the perfectly conducting grating with periodic surface were published for TM and TE polarizations separately with sinusoidal groove profiles and for TM and TE with comb groove profiles. Some experimental results for the comb groove grating were presented by Jull and Ebbeson [16].

The first analysis of the rectangular groove profile was by Wirgin [22] for TM and TE polarization. Some numerical values for simultaneous blazing in both polarization with a rectangular groove profile were published by Hessel et al [14], and Heath and Jull obtained complete data for simultaneous blazing under the Bragg. angle condition, of which only some examples were published in [17].

Although it is clear that the Bragg condition is one condition for the perfect blazing of the conducting gratings with the periodic surface, it is not a necessary condition. Based on the fact that a perfect blazing violating the Bragg condition had never been found, Hessel et al [14], in their remarkable blaze studies, state

1) only two space harmonics propagate; 2) the dimensions of the gratings must satisfy the Bragg condition (i.e. the Littrow mount only) as necessary conditions for perfect blazing. Wirgin [22] seemed to have obtained perfect blazing while violating condition 1, however, it was shown that it was not perfect blazing. So, the Bragg condition was regarded as a necessary condition for perfect blazing until perfect blazing off Bragg angle for TM polarization with rectangular groove profile was reported by Heath, Beaulieu and Jull [11,12] and by Beaulieu in [13].

Only isolated data were reported in [11,12,13], and no theoretical explanation was given for this interesting property. In 1981, Maystre and Cadilhac [19] theoretically predicted this surprising property for a conducting grating with sinusoidal profile : a perfect blazing (an efficiency of 100% in the principal backscatter) can obtained without using Littrow mount. Thus the Bragg condition is not a necessary condition for perfect blazing with sinusoidal gratings. A single example of such perfect blazing for TM polarization with sinusoidal grating was presented in the same paper. This was followed by an example for echelette and rectangular profiles [21].

Furthermore, according to the equivalence rule [18] between the sinusoidal, ruled and rectangular gratings, one may also predict that such perfect blazing (off Bragg angle) exists for other types of periodic profile gratings. So, the earlier works [11,12,13] were recalled, and become the motivation of the study of this thesis.

The object of this thesis is to further investigate the existence of off Bragg angle blazing with the rectangular gratings, Some basic properties of such perfect blazing will be shown. After exhaustive numerical calculation, the design curves are drawn and analyzed.

Here we give the basic equations to study the problems of scattering by a periodic structure, and a review of the literature on the perfect blazing of the periodic gratings.

In Chapter 2, the numerical technique for analyzing the scattering field with rectangular profile gratings, mode matching across the interface between the free space region and waveguide region is again presented.

In Chapter 3, combining the scattering matrix technique [19] and the mode matching method[14], we predict the existence of off Bragg angle blazing with the rectangular gratings. Furthermore, some particular characteristics for such perfect blazing are also derived in this chapter.

Perfect blazing for TM polarization with different rectangular gratings off the Bragg angle is reported in chapter 4. Design curves are plotted in the same chapter. Included also in chapter 4 is an analyses of the numerical solution of the problem.

In Chapter 5 verification, conclusions and recommendations for future studies are given .

Chapter 2. Mode Matching Method

§2.1 Introduction

Only a very limited number of waveguide grating diffraction problems can be solved exactly, and most solutions depend on numerical computation. Mode matching is one method for such problems, and is very useful when the geometry of the structure can be described as a junction of two regions, and each of them independently gives a set of well-defined solutions of Maxwell's equations satisfying the boundary conditions. It also permits the study of deep groove gratings.

Commonly, there are three steps included in the mode matching procedure. First the expansion of the fields in the individual regions in terms of their respective normal modes, so the problem is reduced to determining the set of modal coefficients in the expansions of the electromagnetic fields. Next, by using the boundary conditions at the junction of regions, we can get an infinite set of linear simultaneous equations for the unknown modal coefficients. Finally, applying the orthonormal property of the modes and truncating the infinite set of linear equations , we can get a solution to the problem.

Because approximate techniques (truncation) are used in the mode matching method, the accuracy of the approximated results should be verified carefully.

In this chapter, the problem of scattering with perfectly conducting rectangular gratings by the incident plane electromagnetic wave which is perpendicular to the groove axis is solved by using a mode matching method. The procedure which follows is due to Hessel et al in [14] and was used by Heath in [10] and Michelson in [8].

The coordinate system is shown in Fig 2.1, with the dimensions of grating including width a, depth h, and period d.

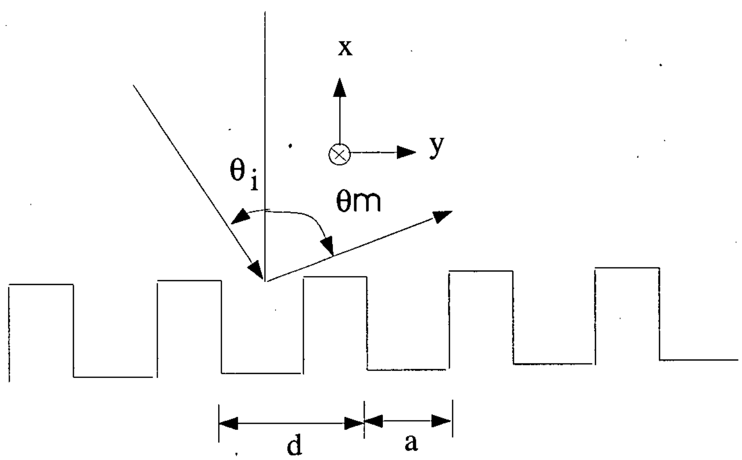

Figure 2.1 Coordinate system of the problem for scattering with a conducting rectangular grating

§2.2 TM Polarization

§ 2.2.1 Expansion of the Fields

A TM polarized plane wave is incident on a grating shown as Fig2.1, with the incidence perpendicular to the groove axis, so that only a $\hat{z}$ component of the magnetic fields exists. Assuming that the time dependence is $\exp(j\omega t)$, and using the Rayleigh expansion for the scattered field H_z^d in the free space region (x>0), the tangential component of the magnetic fields ($H_z^t = H_z^i + H_z^d$) in free space becomes:

$$H_z(x,y) = A_i e^{jk\cos\theta_i x} f_0 + \sum_{m=-\infty}^{\infty} A_m e^{-jk\cos\vartheta_m x} f_m \tag{2.1}$$

where

$$f_m = \frac{1}{\sqrt{d}} e^{-jk\sin\theta_m y} \tag{2.2}$$

$$\begin{aligned} \cos\theta_m &= \sqrt{1-\sin^2\theta_m} & \quad |\sin\theta_m| \leq 1 \\ &= -j\sqrt{\sin^2\theta_m - 1} & \quad |\sin\theta_m| > 1 \end{aligned} \tag{2.3}$$

The functions f are chosen as normal modes in free space for both TM and TE polarization, and $\sin\theta_m$ satisfies the grating formula in (1.1). The value of $\cos\theta_m$ should be either positive real or negative imaginary. The positive real value represents a propagating plane wave, and the negative imaginary represents an evanescent wave ($A_m e^{-k\sqrt{\sin^2\theta_m - 1}} f_m$) which propagates in the y-direction and is exponentially damped in the x-direction.

By applying the Maxwell equation $E_y(x,y) = \frac{j\eta_0}{k}\frac{\partial H_z}{\partial x}$ to equation 2.1, the tangential components of the electric fields in the free space are given as:

$$E_y(x,y) = -A_i\eta_0\cos\theta_i e^{jk\cos\theta_i x} f_0 + \sum_{m=-\infty}^{\infty} A_m\eta_0\cos\theta_m e^{-jk\cos\theta_m x} f_m \tag{2.4}$$

where $\eta_0 = \sqrt{\frac{\mu_0}{\epsilon_0}}$ is the characteristic impedance of free space.

In the waveguide region (groove region), because of the transverse boundary, the fields are in the form of standing waves that have a node at x=-h. In the waveguide, the electric and magnetic fields are given by [14]:

$$H_z(x,y) = \sum_{n=0}^{\infty} C_n \frac{\cos\left(k_n(x+h)\right)}{\cos k_n h} g_n \tag{2.5}$$

$$E_y(x,y) = \sum_{n=0}^{\infty} -jC_n \frac{\eta_0}{k} k_n \frac{\sin\left(k_n(x+h)\right)}{\cos k_n h} g_n \tag{2.6}$$

where

$$\begin{aligned}
g_n &= \sqrt{\frac{\epsilon}{a}} \cos\left(\frac{n\pi\left(x+\frac{a}{2}\right)}{a}\right) \\
k_n &= \sqrt{k^2 - \left(\frac{n\pi}{a}\right)^2} \qquad \left|\frac{n\pi}{a}\right| < k \\
&= -j\sqrt{\left(\frac{n\pi}{a}\right)^2 - k^2} \qquad \left|\frac{n\pi}{a}\right| > k \\
\epsilon &= 1, \qquad n = 0, \\
&= 2, \qquad n = 1, 2, 3, ...
\end{aligned}$$

the functions g_n are normal mode in amplitude the groove region for both TM and TE polarizations.

§2.2.2 Mode Matching

The x=0 plane is the junction between the free space and groove regions. The boundary conditions are:

$$
\begin{aligned}
H_z(0^+,y) &= H_z(0^-,y) & |y| < \frac{a}{2} \\
H_z(0^+,y) &= -J_y(0,y) & \frac{a}{2} < |y| < \frac{d}{2}
\end{aligned}
\tag{2.7}
$$

where J_y is the surface current density, and

$$
\begin{aligned}
E_y(0^+,y) &= E_y(0^-,y) & |y| < \frac{a}{2} \\
E_y(0^+,y) &= 0 & \frac{a}{2} < |y| < \frac{d}{2}
\end{aligned}
\tag{2.8}
$$

We now apply the boundary condition by mode matching the tangential electric and magnetic fields in both regions across the plane x=0. Substituting (2.1) (2.5) into (2.7), we have:

$$
A_i f_0 + \sum_{m=-\infty}^{\infty} A_m f_m = \sum_{n=0}^{\infty} C_n g_n \tag{2.9}
$$

For simplicity, we redefined $A_0 = A_i + A_{ref}$ where A_i and A_{ref} (formerly A_0 in (2.1) (2.5))are the complex coefficients of the incident wave and of the specularly reflected wave respectively. Then equation (2.7) becomes:

$$\sum_{m=-\infty}^{\infty} A_m f_m = \sum_{n=0}^{\infty} C_n g_n \tag{2.10}$$

and, substituting (2.4) (2.6) into (2.8), we have the other equation:

$$\begin{aligned} -2A_i \cos\theta_i f_0 + \sum_{m=-\infty}^{\infty} A_m \cos\theta_m f_m &= \sum_{n=0}^{\infty} C_n \frac{k_n}{jk} \tan(k_n h) g_n, \quad |y| < \frac{a}{2} \\ &= 0 \qquad \frac{a}{2} < |y| < \frac{d}{2} \end{aligned} \tag{2.11}$$

§2.2.3 Solution

Defining the inner products of the normal modes as:

$$\langle f_m, g_n \rangle = \int_{-\frac{d}{2}}^{\frac{d}{2}} f_m \cdot g_n^* \cdot dx \tag{2.12}$$

and from the orthonormal property of the normal modes, we have:

$$\begin{aligned} \langle f_m, f_n \rangle &= \delta_m^n \\ \langle g_m, g_n \rangle &= \delta_m^n \end{aligned} \tag{2.13}$$

where δ is Kronecker delta.

The inner product of both sides of equation (2.10) with g_n, gives us the representation of groove mode coefficient C_n in terms of A_m:

$$\sum_{m=-\infty}^{\infty} A_m \langle f_m, g_n \rangle = C_n \tag{2.14}$$

Similarly, the inner product of both sides of equation (2.11) with $f_m$gives:

$$-2A_i \cos\theta_i \delta_m^0 + A_m \cos\theta_m = \sum_{n=0}^{\infty} C_n \frac{k_n}{jk} \tan(k_n h) \langle g_n, f_m \rangle \tag{2.15}$$

For two independent equations (2.14) and (2.15), we have two ways of solving for the unknown coefficients A_m . Instead of substituting one equation onto the other, considering the cost of computation time, we chose the following indirect procedure as the way to get the coefficients of the free space modes.

First, substituting (2.15) into (2.14) gives us:

$$\sum_{m=-\infty}^{\infty}\left(\sum_{n'=0}^{\infty} C_{n'}\frac{k_{n'}}{jk}\frac{\tan(k_{n'}h)}{\cos\theta_m}\langle g_{n'},f_m\rangle + 2A_i\delta_m^0\right)\langle f_m,g_n\rangle = \sum_{n'=0}^{\infty} C_{n'}\delta_n^{n'} \tag{2.16}$$

for convenience, and by some rearranging steps, the equation (2.16) can be written in the form of the matrix equation as:

$$\left(\left[C'\right]\left[B'\right]+\left[G'\right]\right)X = F' \tag{2.17}$$

where:

$$C'_{nm} = \langle f_m, g_n\rangle$$

$$B'_{mn'} = \frac{k_{n'}}{jk\cos\theta_m}\langle g_{n'}, f_m\rangle$$

$$G'_{nn'} = -\delta_{n'}^{n} k_{n'} cot k_{n'} h$$

$$X_{n'} = C_{n'}\tan k_{n'}h$$

$$F'_n = -2A_i\langle f_0, g_n\rangle$$

and finally, the solution of A, can be given by applying equation (2.15) as:

$$A = \left[B'\right]X + 2A_i\delta_m^0 \tag{2.18}$$

§2.3 TE Polarization

When a TE polarized plane wave is incident on the same grating shown as Fig2.1, with the incidence perpendicular to the groove axis, so that only a component of the electric field exists, the tangential components of both electric and magnetic fields in the free space , x> 0 , are given by:

$$E_z(x,y) = B_i e^{jk\cos\theta_i x} f_0 + \sum_{m=-\infty}^{\infty} B_m e^{-jk\cos\theta_m x} f_m \tag{2.19}$$

$$H_y(x,y) = \frac{B_i \cos\theta_i}{\eta_0} e^{jk\cos\theta_i x} f_0 - \sum_{m=-\infty}^{\infty} \frac{B_m \cos\theta_m}{\eta_0} e^{-jk\cos\theta_m x} f_m \tag{2.20}$$

and the tangential components of fields in the groove region are given as:

$$E_z(x,y) = \sum_{n=1}^{\infty} D_n \frac{\sin(k_n(x+h))}{\sin k_n h} g_n^{'} \tag{2.21}$$

$$H_y(x,y) = \sum_{n=1}^{\infty} -jD_n \frac{k_n}{k\eta_0} \frac{\cos(k_n(x+h))}{\sin k_n h} g_n^{'} \tag{2.22}$$

where $g_n^{'}$ is the normal modes for TE polarization in the groove region :

$$g_n^{'} = \sqrt{\frac{2}{a}} \sin\left(\frac{n\pi(y+\frac{a}{2})}{a}\right)$$

The boundary conditions in x=0 plane are:

$$\begin{aligned}
&H_y(0^+,y) = H_y(0^-,y), && |y| \leq \frac{a}{2} \\
&H_y(0^+,y) = J_z(0,y), && \frac{a}{2} \leq |y| \leq \frac{d}{2} \\
&and && \\
&E_z(0^+,y) = E_z(0^-,y), && |y| \leq \frac{a}{2} \\
&E_z(0^+,y) = 0, && \frac{a}{2} \leq |y| < \frac{d}{2}
\end{aligned} \tag{2.23}$$

Following the same steps described above for TM polarization, and redefining $B_0 = B_i + B_{ref}$ for the same reason as before, the unknown coefficients of B can be given from the solution of following matrix equations:

$$\left(\left[B'\right]\left[C'\right] + \left[G'\right]\right)X' = F' \tag{2.24}$$

where:

$$B'_{nm} = \left\langle f_m, g'_n \right\rangle$$

$$C'_{mn} = jk\cos\theta_m \left\langle g'_n, f_m \right\rangle$$

$$G'_{nn'} = \delta_n^{n'} k_n cot(k_n h)$$

$$X'_n = D_n$$

$$F'_n = 2B_i jk\cos\theta_i \left\langle f_0, g'_n \right\rangle$$

and

$$B_m = \frac{1}{jk\cos\theta_m}\left[B'\right]X'$$

§2.4 Validity of Numerical Solutions

The numbers of both free space and groove modes in equations (2.17) and (2.24) are infinite, so, they should be truncated into a definite number M and N respectively before the matrix equations can be solved, because of the finite computer capacity. This raises the problem of verification of the numerical results.

Normally there are three ways used to verify the numerical results besides the using of experimental results: checking conservation of energy, reciprocity and convergence. According to the analysis given before, for the problem of a diffraction grating, conservation of energy in the free space region can be expressed as:

$$|A_i|^2 \cos\theta_i = \sum_m |A_m|^2 \cos\theta_m \tag{2.25}$$

and the summation includes only those free space propagating harmonics. But, unfortunately according to the result given by Hessel et al in [14], it can be shown that energy conservation is independent of the truncation used. Thus conservation of the energy, while necessary, can not be used here as a sufficient check of the accuracy of the solution. However, conservation of the energy is used in our program mainly to indicate the error information produced by the problems in coding or excessive round-off during computation.

The reciprocity in our problem can be generally described as [1] : The efficiency in the mth order does not change when the grating is rotated by 180^0 about an axis perpendicular to the plane on which it has been ruled. Furthermore, the special property of the reciprocity in our topic will be discussed in detail in following chapter. But unfortunately it is not a sufficient condition for the validity of out numerical solution either.

A series can be truncated only if it is convergent or at least semi-convergent. A traditional way that plots the numerical values of some desired parameters versus the number of terms retained meets its limitation here, for the reason that to use the mode matching method, we need to truncate two or more infinite series simultaneously. The numerical results may converge to different values depending on the way we truncate the two series, which is called " relative convergence", and the ratio of waveguide modes to free space modes N/M can be as important as the values of N and M.

Values of the reflection efficiency of a selected grating ($a/d=0.5$, $d/\lambda=0.87, h/\lambda=0.231$) so that only specular reflected ($m=0$) and principal backscattering ($m=-1$) modes exist, are shown in Fig 2.2 as a function of the number of free space modes M, with different N/M ratios. In all cases the grating is illuminated perpendicular to the groove axis with the Bragg angle as the incident angle.

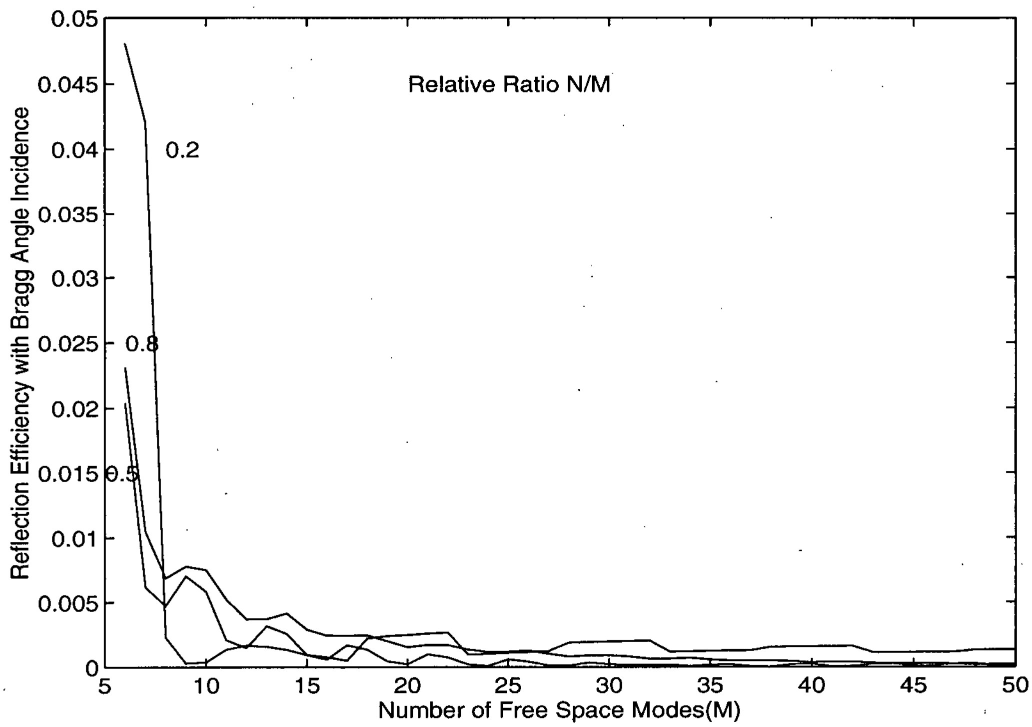

Figure 2.2 Convergence of the reflection efficiency for Bragg angle incidence with the number of the free space modes with a/d=0.5, $d/\lambda=0.87$, $h/\lambda=0.231$

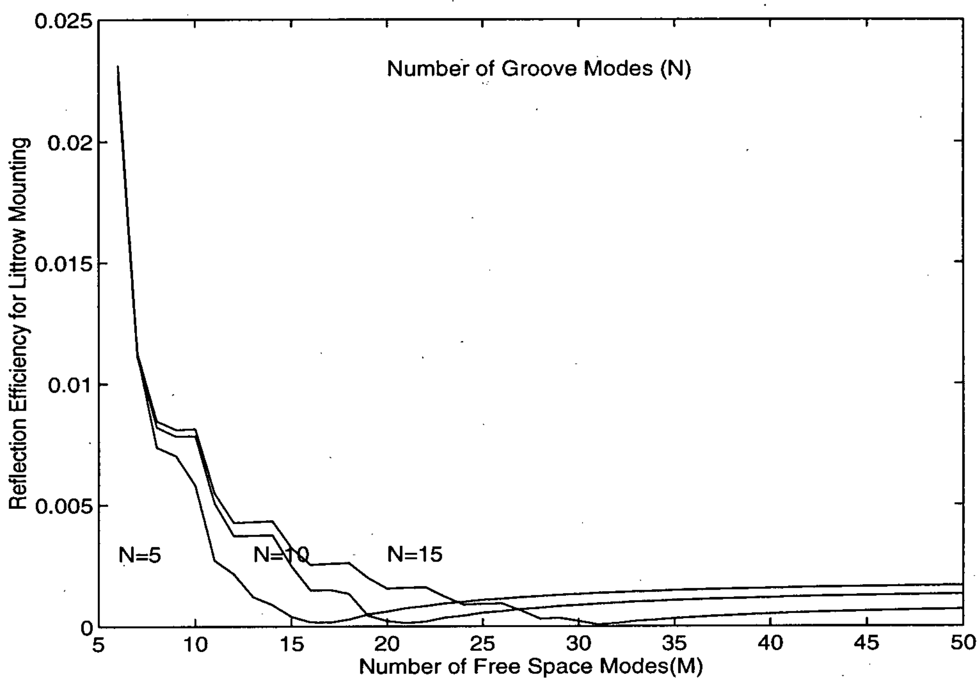

Figure 2.3 Convergence of the reflection efficiency with the number of free space modes for TM polarization for a/d=0.5 d/λ=0.87, h/λ=0.231

From Fig 2.2, it can be seen that the numerical results given from equation (2.18) fortunately suffer very little from the relative convergence phenomena, which means that the method we use in this thesis is quite reasonable.

Now, how to choose the ratio of groove modes N to free space modes M becomes a question. From Fig 2.3 in which we keep the groove modes N unchanged, it can be seen that the numerical value converges monotonically when the ratio of groove modes to space modes reaches about the point which equals the aspect ratio (a/d=0.5 in this example) but, when we continue to increase the value of the M, the results are influenced by relative convergence. Also from Fig2.2, compared with other curves with different N/M ratios, the N/M=0.5 curve drops quite abruptly, and converges at the small value of M. So, it is supposed that the optimum value of the ratio N/M can be chosen about as same as the value of the aspect ratio of the grating, which agrees with other studies reported by Michelson in his PhD thesis[8] .

Because the computer time used to solve an (m,m) matrix is proportional to m^3, according to the conclusion we derived from figure 2.2 and figure 2.3, we can use smaller values of M and N than those large values chosen by Hessel et al (for example, Hessel et al [14] and Heath [10] used M=50 and N=10 for all dimensions of the gratings). Thus the computation used for the results in the following chapters can proceed efficiently.

Chapter 3. Off Bragg Blazing With Rectangular Gratings

§3.1 Introduction

The Bragg angle condition seems no longer a necessary condition for the perfect blazing, after the earlier reports [11,12,13] and reports of perfect blazing in a non-zero deviation mounting (i.e. without using the Bragg condition) with sinusoidal, echelette and symmetrical rectangular profiles for the TM polarization were published in 1981 by Maystre et al[19] and [21] in 1981. No other papers on this surprising phenomenon appear to have been published since then.

In this chapter, using the scattering matrix technique combined with an adequate coordinate translation used by Maystre et al [19], the possibility of the existence of such off Bragg angle blazing is shown. Furthermore, according to the "equivalence rules" proposed by Maystre et al [18], such blazing exists in the ruled and sinusoidal gratings[21]. Using the reciprocity theorem and results given before, the dimensions of rectangular gratings for off Bragg angle blazing is discussed.

§3.2 The Off Bragg Angle Blazing

In this section we restrict our discussion to the situation in which only two propagating orders are diffracted (i.e. the specular reflection m=0 and the principal backscattering m=-1), and we adopt the coordinate system used before (fig 2.1)

Assuming a TM polarized plane wave illuminates the grating at an angle of incidence of θi, because of the assumption of only two orders of diffraction, we get two propagating diffraction waves at the diffraction angles $\theta_0 = \theta_i$ and θ_{-1}. The incident field, from equation 2.1, becomes $H^i = A_i exp(jk(x\cos\theta_i - y\sin\theta_i))$where A_i is a complex amplitude coefficient.

Taking into account reciprocity , an incident wave illuminating the grating under the incidence of θ_{-1} also generates two diffracted propagating orders at diffraction angles $\theta_0$and θ_{-1}. So, to set up the scattering matrix, we assume that two incident waves with coefficients A_1 and A_2 incident at $\theta_1 = \theta_0$ and $\theta_2 = \theta_{-1}$ respectively, illuminate the grating, the total incident field becomes:

$$H^i = A_1(exp(jk(x\cos\theta_1 - y\sin\theta_1))) + A_2(exp(jk(x\cos\theta_2 - y\sin\theta_2))) \quad (3.1)$$

By assuming the complex coefficients of the diffraction orders as B_1, B_2, the diffraction fields can be written as:

$$H^d = B_1(exp(-jk(x\cos\theta_1 + y\sin\theta_1))) + B_2(exp(-jk(x\cos\theta_2 + y\sin\theta_2))) \quad (3.2)$$

By denoting the complex vectors: $\hat{a} = \left(A_1\sqrt{\cos\theta_1}, A_2\sqrt{\cos\theta_2}\right); \hat{b} = \left(B_1\sqrt{\cos\theta_1}, B_2\sqrt{\cos\theta_2}\right)$the scattering matrix S can be set as:

$$S = \begin{bmatrix} S_{11} & S_{12} \\ S_{21} & S_{22} \end{bmatrix} \quad (3.3)$$

where, the component of the element of S, S_{mn}, represents the complex reflection coefficient for the mth order diffraction wave which is excited by the nth incident wave. The S matrix, which depends on both the dimension of the grating and the characteristics of the incident waves such as the wave length and the angle of incidence, can be calculated by the means of the mode matching method outlined in last chapter.

But, four complex coefficients of the S matrix are quite difficult to analyze. So, in the remainder of the section, we reduce these complex coefficient to real ones by the means of a coordinate translation.

Assuming the new coordinate system given by:

$$\begin{aligned} x' &= x - \Delta x \\ y' &= y - \Delta y \\ z' &= z \end{aligned} \tag{3.4}$$

then, by using equations (3.1) (3.2), we can get the new vectors $\hat{a}'$and$\hat{b}'$ and the new S matrix S' can be written from S as:

$$\begin{aligned} S'_{11} &= S_{11} exp(-2jk\Delta x \cos\theta_1) \\ S'_{22} &= S_{22} exp(-2jk\Delta x \cos\theta_2) \\ S'_{12} &= S_{12} exp(-jk\Delta x(\cos\theta_1 + \cos\theta_2)) exp\left(-j\frac{2\pi\Delta y}{d}\right) \\ S'_{21} &= S_{21} exp(-jk\Delta x(\cos\theta_1 + \cos\theta_2)) exp\left(j\frac{2\pi\Delta y}{d}\right) \end{aligned} \tag{3.5}$$

where the phase differences caused by the shifts Δx,Δy are accounted for. From equations (3.5) we can see that:

$$\begin{aligned} \det\left(S'\right) &= exp(-2jk(\cos\theta_1 + \cos\theta_2)\Delta x) \det(S) \\ \frac{S'_{12}}{S'_{21}} &= \frac{S_{12}}{S_{21}} exp\left(-j\frac{4\pi\Delta y}{d}\right) \end{aligned} \tag{3.6}$$

If we adopt an appropriate coordinate translation, by carefully choosing Δx and Δy, we can get a particular matrix S', denoted as U, so that:

$$\begin{aligned} \det(U) &= 1 \\ \frac{U_{12}}{U_{21}} &= 1 \end{aligned} \tag{3.7}$$

Equations (3.7) can be used to calculate the value of Δx and Δy. Now, U becomes the matrix that is symmetrical, unitary with determinant 1. Taking into account an elementary property of linear algebra, U can be expanded by a symmetrical and Hermitian matrix A in terms of:

$$U = exp(jA) = I + jA + \frac{(jA)^2}{2!} + ... + \frac{(jA)^n}{n!} + ... \tag{3.8}$$

Because det(U)=1, trace(A) may be zero, A takes the simple form:

$$A = \begin{bmatrix} \gamma & \beta \\ \beta & -\gamma \end{bmatrix} \tag{3.9}$$

with real parameters β and γ. If we rewrite the real parameters β and γ in the form of another two real numbers ρ and α by γ=ρcosα and β=ρsinα, then:

$$A = \rho A' = \rho \begin{bmatrix} \sin\alpha & \cos\alpha \\ \cos\alpha & -\sin\alpha \end{bmatrix} \tag{3.10}$$

Because $A'^2 = I$ then

$$\begin{aligned} U &= I + j\rho A' - \frac{\rho^2 I}{2!} - \frac{j\rho^3 A'}{3!} + \frac{\rho^4 I}{4!} + ... \\ &= I\cos\rho + jA'\sin\rho \end{aligned} \tag{3.11}$$

$$U = \begin{bmatrix} \cos\rho + j\sin\rho\sin\alpha & j\sin\rho\cos\alpha \\ j\sin\rho\cos\alpha & \cos\rho - j\sin\rho\sin\alpha \end{bmatrix} \tag{3.12}$$

Now, taking into account the reciprocity theorem described in chapter 1, under the Bragg angle condition and considering the specular reflection wave (m=0) only, we can get a quite simple result as $S_{11} = S_{22}$. From (3.12) for this we can choose α=0 or ρ=0. Because when ρ=0, $U_{12} = U_{21} = 0$, so, generally we should choose α=0 for the Bragg angle condition.

On the other hand for the case of arbitrary dimensions of the grating, from equation 3.12, it is interesting to see that the diffraction efficiency of the principal backscatter order (m=-1), or the ratio of the power in the m=-1 order to the incident power, is

$$E^{-1} = \sin^2 \rho \cos^2 \alpha \tag{3.13}$$

So, to obtain a perfect blazing, generally two conditions should be satisfied simultaneously as:

$$\begin{aligned} \rho &= n\pi + \frac{\pi}{2} \\ \alpha &= m\pi \end{aligned} \tag{3.14}$$

where n and m are integers.

Combining this S matrix technique above of Maystre et at [19] with the mode matching method outlined in detail in the previous chapter, we developed our program to find perfect blazing without satisfying the Bragg angle condition.

Defining the deviation$D = |\theta_1 + \theta_2|$, where θ_1 is incident angle while θ_2 is the diffraction angle for backscatter order (when the Bragg angle condition is satisfied, D should be zero). We draw a set of parametric curves giving ρ (in obsicissa) and α (in ordinate) as functions of d/λ for various deviations . As an example, we made our calculation for the gratings with the dimensions as a/d=0.5,h/d=0.25. The result for TM polarization is given in fig 3.1. The curve met the point of α=π,ρ=π/2, for d/λ is chosen as about 0.92, and the deviation is chosen as 19.8^0 ($\theta_1 = 23.7^0, \theta_2 = -43.5^0; \theta_1 = 43.5^0, \theta_2 = -23.7^0$), and the behavior of the reflection efficiency at this point is shown in figure 3.2.

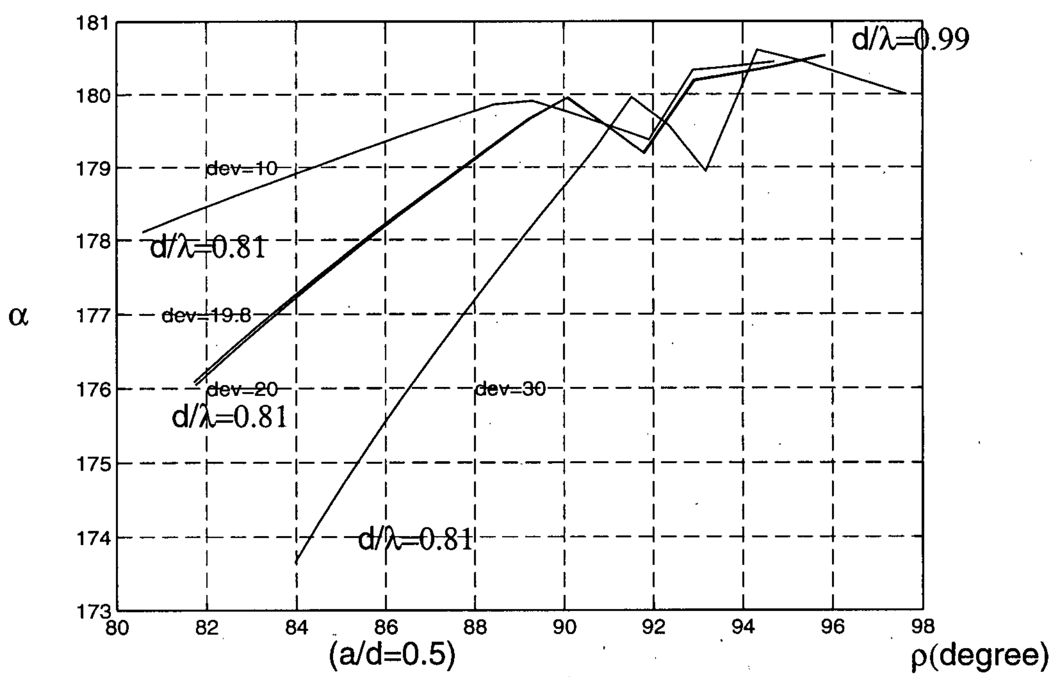

Figure 3.1 Parametric curves of d/λ for various deviations (a/d=0.5)

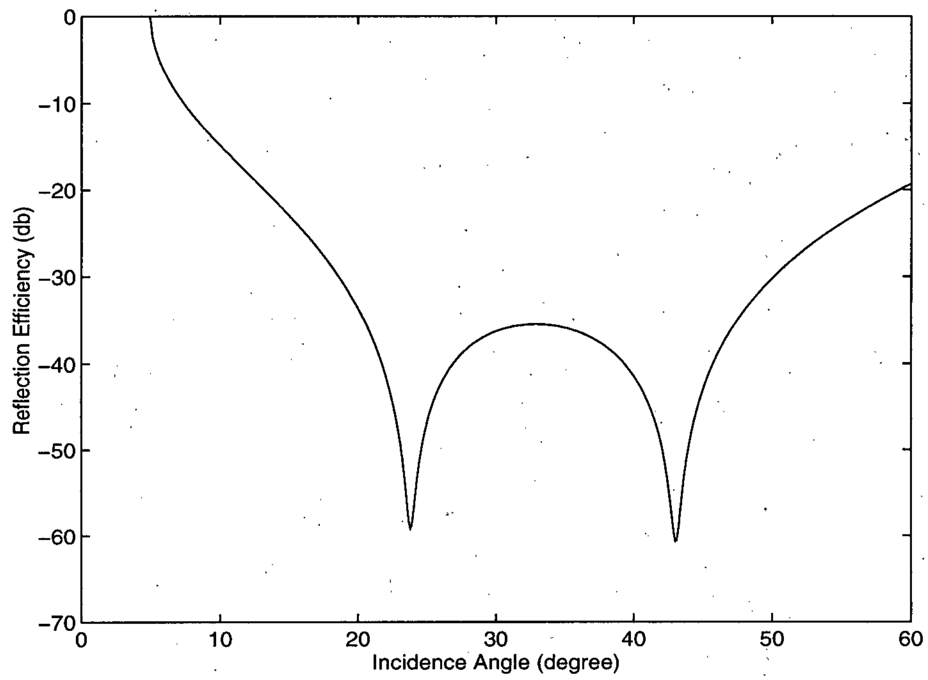

Figure 3.2 Reflection efficiency as a function of the angle of the incidence, with a/d=0.5,h/d=0.25,d/λ=0.92, dev=19.8

It is quite interesting to analyze the properties shown in figure 3.1 and to find out the possibility of the occurrence of off Bragg angle blazing. First, the curves drawn in fig. 3.1 are quite similar with the curves published by Maystre et al [19] for TM polarization with sinusoidal gratings, which satisfies what the equivalence rules described. For D=10, the curve first approaches the α=π line at the point of $\rho < 90^0$; then we increase D=20, and the curve almost meets the perfect blazing point (α=π,ρ=π/2); Finally, we continue to increase D=30, the first intersection of the curve and the line of α=π passes the perfect blazing point at the point about $\alpha = 91.7^0$. So, it is very easy for us to conclude that perfect blazing may occur near D=20. At last, under the accuracy which our calculation program can provide, we find the perfect blazing occurs at $D = 19.8^0$ which is proven by figure3.2.

Now, choosing another dimension of the grating arbitrarily, with a/d=0.5, and keeping h unchanged as h/λ=0.206, we draw another set of parametric curves for TM polarization given in figure 3.3. From the figure perfect blazing may be obtained at the point of D=52.8, d/λ=0.99, which can be displayed in detail in the reflection efficiency curve in figure 3.4.

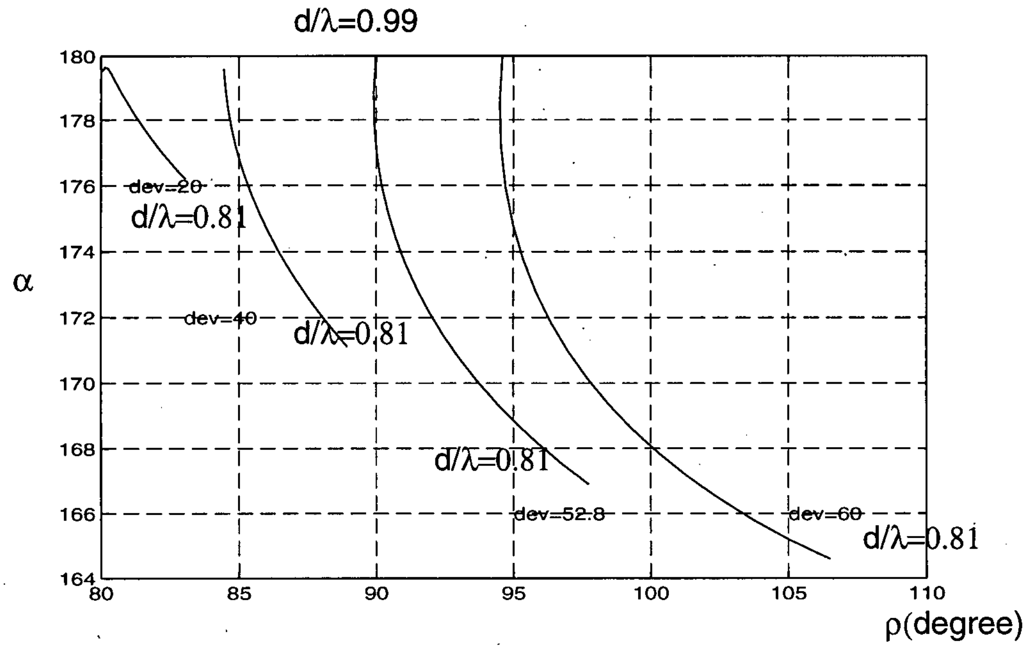

Figure 3.3 Parametric curves of d/λ with a/d=0.5,h/λ=0.206

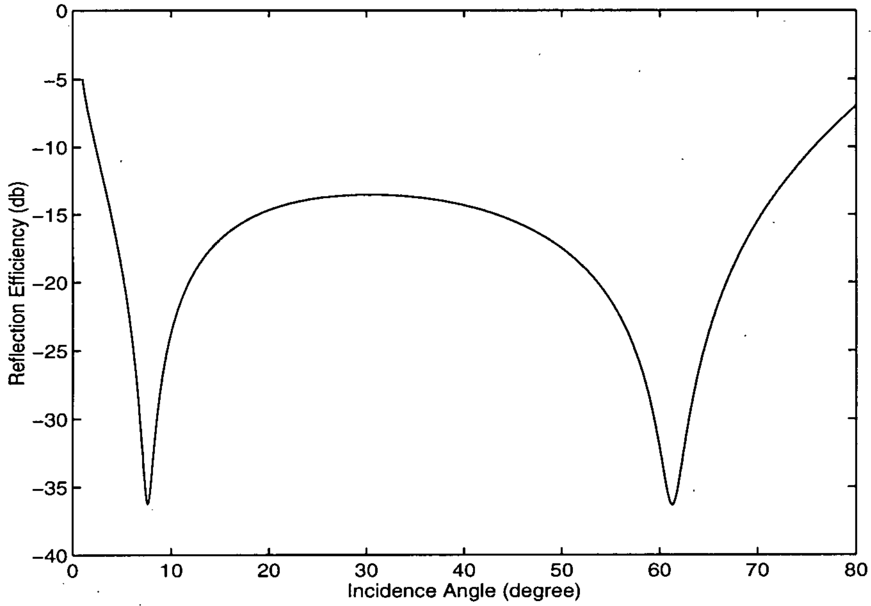

Figure 3.4 Reflection efficiency as a function of the incidence angle for a/d=0.5, h/λ=0.206,d/λ=0.99

In figure 3.3, it is interesting to see that, as deviation D increases, the intersection of the curves with the line $\alpha=\pi$ moves towards the point of $\rho=\pi/2$. When D is chosen as 52.8^0, the curve meets the perfect blazing point at $\alpha=\pi,\rho=\pi/2$. And if we increase further the values of deviation, the curves move away from this perfect blazing point.

So, from figure 3.1 and figure 3.2, we can conclude that perfect blazing may be obtained while the Bragg angle condition is not satisfied, at least in the case of the TM polarization with conducting symmetrical rectangular gratings.

Because the first theoretical prediction of off Bragg angle blazing was published with sinusoidal gratings, and only between the sinusoidal and the symmetrical rectangular (a/d=0.5) gratings there exists the equivalence rules which will be described in detail in Appendix A.1, until now, we restrict our discussion within the range of the symmetrical rectangular gratings.

But, as can be shown from the examples of figure 3.1 and figure 3.2, the dimensions of the grating can be chosen quite arbitrarily. We can expect that such off Bragg angle blazing may occur for other dimensions of symmetrical rectangular gratings, further more, it can also be expected that such perfect blazing may occur for ordinary rectangular gratings (a/d not equal to 0.5). This is the motivation and main topic of the research in next chapter.

§3.3 The Range for Off Bragg Blazing

Now that we shown the possibility of off Bragg angle blazing, to define the range where such perfect blazing may occur becomes quite important for the following discussion and calculation.

From figure 3.2 and figure 3.4, we can conclude that: Assuming only two orders of diffraction occur (m=0, m=-1), if off Bragg angle blazing can be found, it will be found in pairs of angles, which can be shown immediately by taking into account reciprocity [12].

Let's consider the situation when such blazing occurs, with reference to

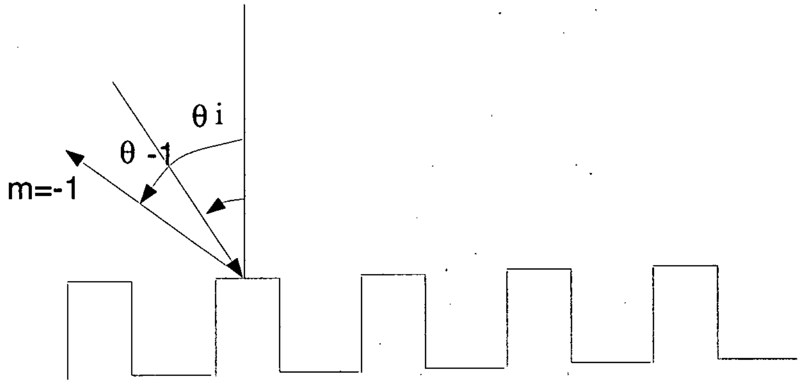

figure3.5: Figure 3.5 Off Bragg Blazing

When a plane wave illuminates the grating with incidence of θi as shown in figure 3.5, assuming the diffraction angle of the principal backscatter is θ_{-1}, according to the elementary grating formula, there exists the relationship between these two angles as:

$$\sin\theta^1_{-1} = \sin\theta^1_i - \frac{\lambda}{d} \tag{3.15}$$

where the superscript 1 represents the first incidence. When the plane wave illuminates the same grating with incidence of $\theta^2_i = -\theta^1_{-1}$, we can get another equation:

$$\sin\theta^2_{-1} = \sin\theta^2_i - \frac{\lambda}{d} \tag{3.16}$$

Taking into account the reciprocity theorem, it can be written immediately that:

$$\begin{aligned} \theta^2_i &= -\theta^1_{-1} \\ \theta^2_{-1} &= -\theta^1_i \end{aligned} \tag{3.17}$$

substituting the equations (3.17) into (3.15), we can get a very useful equation:

$$\sin\theta_i^1 + \sin\theta_i^2 = \frac{\lambda}{d} \tag{3.18}$$

also, the equation 3.17 was verified by figure 3.2 3.4, which means that the off Bragg angle blazing angles may occur in pairs. For convenience, we redraw figure 1.1 here to show the shaded region in which off Bragg angle blazing can occur.

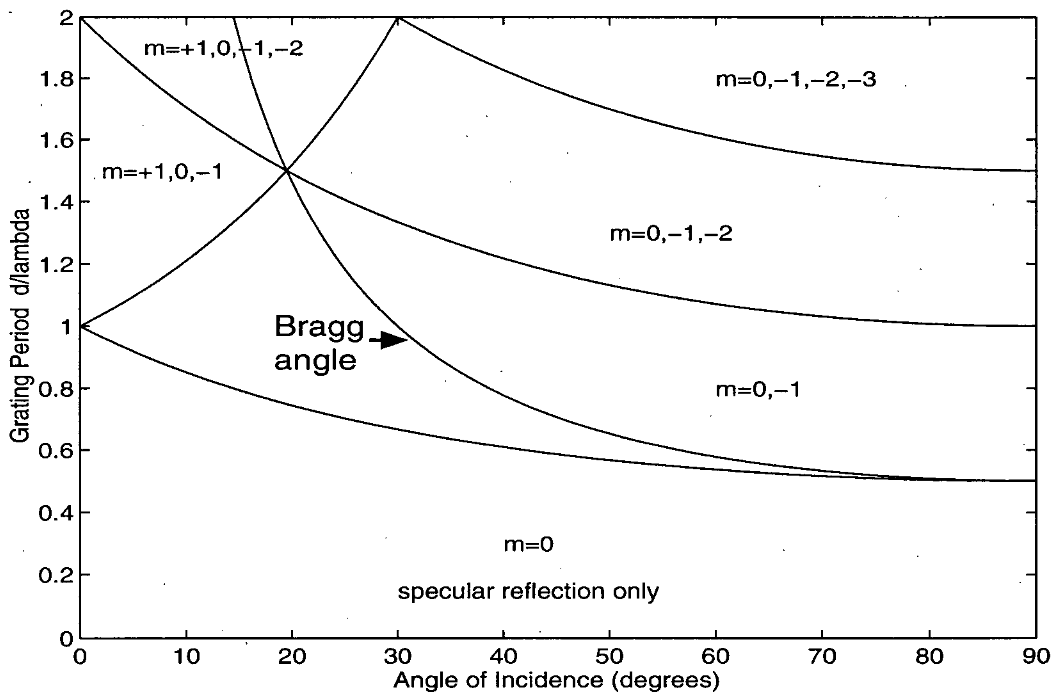

Figure 1.1: Propagating diffraction orders as a function of the grating period and the angle of incidence. Off Bragg blazing angles may occur in pairs on opposite side of the Bragg angle curve in the shaded region

Combining the Bragg angle condition with equation 3.17, we can get the relationship between them as:

$$\sin\theta_i^2 - \sin\theta_{Bragg} = \sin\theta_{Bragg} - \sin\theta_i^1 \tag{3.19}$$

where θ(Bragg) satisfies the Bragg angle condition $\sin\theta_{Bragg} = \frac{\lambda}{2d}$.

Equation (3.19) tells us that θ_i^1 and θ_i^2 should be on opposite sides of the Bragg angle respectively, or , in figure 1.1a, one of these two angles should be left of the Bragg angle curve and the other located to the right of the Bragg angle curve.

It is very interesting to find that if one of these two angles is on the left solid curve of $\sin\theta = 1 - \frac{\lambda}{d}$ the other is on the right solid curve of $\sin\theta = \frac{2\lambda}{d} - 1$. Figure 3.6 gives an example of such situation (a/d=0.5, d/λ=1.32,h/λ=0.647). Note that, from figure1.1a, in addition to the m=0,-1 spectral orders, the m=+1 order exists for $\theta_i < \theta_1$and the m=-2 order exists for $\theta_i > \theta_2$

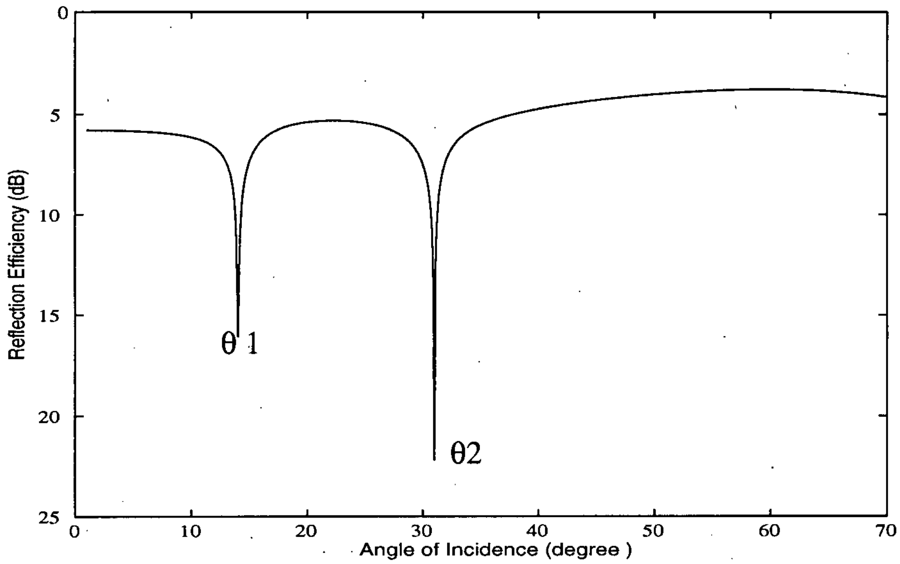

Figure 3.6 Reflection efficiency with a/d=0.5, d/λ=1.32, h/λ=0.647, to demonstrate that sinθ1=1-λ/d, sinθ2=2λ/d-1

We can find off Bragg angle blazing in the whole region where only two propagation orders exist (m=0, m=-1). It is quite interesting to compare our results with those for Littrow mounting. The Bragg angle blazing occurs in the region of $19.5^0 < \theta_i < 90^0$, while the off Bragg angle blazing may occur in the region of $0^0 < \theta_i < 90^0$. However, from figure 1.1, d/λ should be chosen in the same region as that for Littrow mounting (i.e. 0.5<d/λ<1.5).

It is also very interesting to find that if we choose $\theta_i^1 = \theta_i^2$, equation 3.18 becomes the famous Bragg angle condition. So, we can conjecture that the Bragg angle blazing is probably a particular case of off Bragg angle blazing.

Chapter 4. Numerical Results

§4.1 Introduction

As was pointed out in the previous chapter and in earlier works [11,12,13], an occurrence of off Bragg angle blazing for other dimensions than a=0.5d of rectangular gratings is expected. The object of this chapter is to demonstrate our assumption and to find the relations among the dimensions of rectangular gratings for off Bragg angle blazing. Here we will try to extend the single example of off Bragg blazing, used as the evidence of the existence of such perfect blazing , to the whole range of dimensions of the rectangular grating. These may be used for design curves.

There are two difficulties we will meet in our numerical calculation. One of them is that there are few previous research results on this topic to be used as the reference for the verification for our numerical results. The other is that, compared with the numerical calculation for the Bragg angle blazing in which only the angle satisfying the Bragg condition should be checked, here, according to the results of last chapter, for each value of λ/d, all the deviations (0<D<90) should be checked, which means much more extensive calculations.

To overcome the first difficulty, we should always keep in mind during the calculations those conventional methods of verification such as conservation of energy and reciprocity theorem. Fortunately sometimes the comparison of some results obtained previously for Bragg angle blazing with our numerical results may also make them reasonable.

When using the mode matching method to obtain the numerical solution, there is one more variable — deviation should be considered, Because unfortunately there is no simple equation between the deviation and other dimensions of the rectangular grating has been derived, such as the Bragg angle condition used for the Bragg blazing, it requires much more computing time to get numerical results.

However, given the deviation of the incident angle and backscattering angle, the period d, and the wavelength λ, from the definition of deviation:

$$D = |\theta_i + \theta_{-1}| \tag{4.1}$$

and from the Bragg angle condition which is rewritten in equation (4.2)

$$\sin\theta_{-1} = \sin\theta_i - \lambda/d \tag{4.2}$$

we can calculate the angle of incidence from these two equations. In our program, only the case of $\theta_i + \theta_{-1} > 0$ is considered, and we remove the absolute value symbols in equation (4.1). Taking into account the reciprocity theorem we discussed in detail in last chapter, we can obtain the other result by considering $\theta_i^2 = -\theta_{-1}^1$.

For off Bragg blazing , because of all the variables, incidence angle θi, wavelength λ, period d, groove depth h, and width a, are largely independent of each other, and because the total range of the incident angle (from zero to $\pi/2$) should be checked, an exhaustive search may be required here. Generally the range where the off Bragg blazing occurs for the certain value of a/d is defined first, then a more accurate numerical technique will be used to get the exact value.

Following these two steps, in next section, we constrict our discussion on the off Bragg angle blazing for the symmetrical (a=0.5d) rectangular gratings, then we extend our research to other ordinary rectangular gratings. Some of the corresponding design curves are given in the next two sections.

§4.2 Symmetrical Rectangular Gratings

Since the terms involving the groove depth h in equation (2.17) are periodic, keeping other variables (a,d,D and λ) unchanged, it is expected that there exists more than one value of h at which all reflected power is eliminated. For Bragg angle blazing, it has been already discovered that the groove depth dependence is a quasiperiodical function for both TE and TM polarization. It is very interesting to extend such results to our off Bragg blazing situation here.

When we choose a/d=0.5 for the symmetrical rectangular gratings, D as 19.8 degrees, and d/λ=0.917, the similar periodical phenomenon of the groovedepth for the TM polarization is shown in figure 4.1, in which the first perfect blazing point can be verified by figure 3.2.

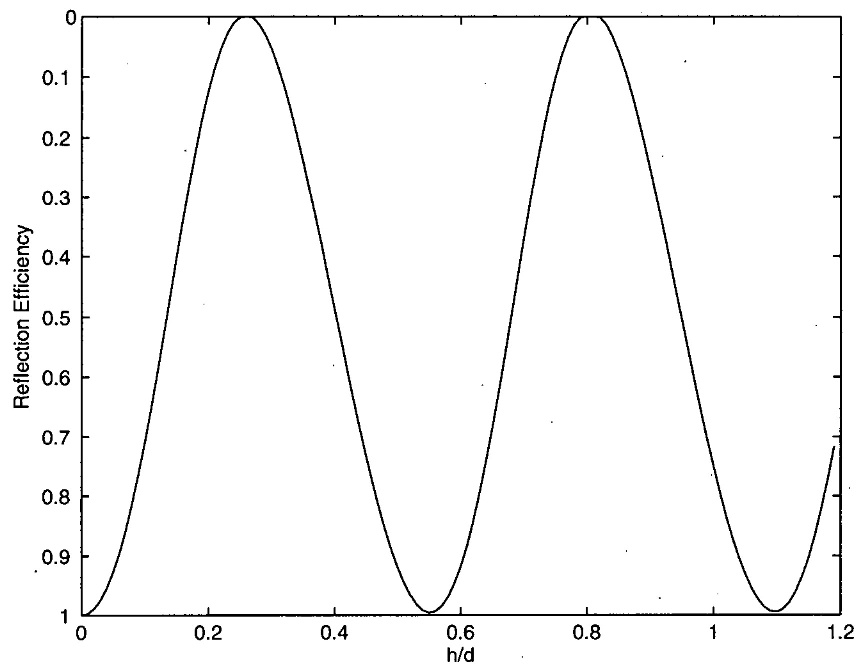

Figure 4.1 Periodicity of the symmetrical rectangular grating with a/d=0.5, D=19.8, d/λ=0.917

Comparing with similar reports published for the Littrow mounting [7] [14], it is quite satisfying to find that the shape of the curve drawn here is very similar to that for Bragg angle blazing. This interesting comparison at least tells us two things. First it confirms the assumption proposed by Maystre in [19] and a similar assumption adopted in the last chapter that " such off Bragg angle blazing may occur for other dimensions of the symmetrical rectangular gratings ". and furthermore, from figure 4.1, it can be seen that if we choose the depth h as the only changing parameter, we can get the off Bragg angle blazing point periodically.

Secondly, such similarity between our results and those for the Littrow mounting may also provide the evidence for our another conjecture in the last chapter that " Bragg angle blazing is probably a particular case for off Bragg angle blazing".

However, for practical reasons such as grating fabrication and frequency bandwidth, usually the shallow gratings are generally used. In the following discussion, we will pay much attention to the shallow gratings i.e., we will discuss in detail the situation when the smallest values of the groove depth are chosen for off Bragg perfect blazing.

For the symmetrical rectangular gratings ($a/d=0.5$), an exhaustive search for the off Bragg angle blazing was made by choosing h/λ and d/λ as the variable parameters and checking the whole range of incident angles for each given h/λ and d/λ. The result is shown in figure 4.2. In figure 4.2, it can be seen that for the TM polarization, perfect blazing (both Bragg and off Bragg blazing) most frequently occurs in the range $0.1<h/\lambda<0.24$ and $0.9<d/\lambda<1.0$.

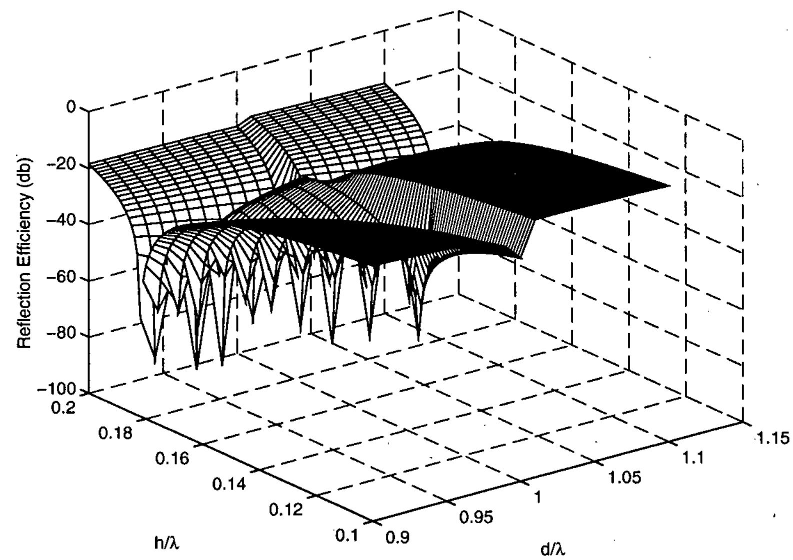

Figure 4.2 Demonstration for the range of the off Bragg blazing (a/d=0.5)

To obtain the exact perfect blazing point, we adopt a more accurate algorithm called golden section search in both h and d dimensions within the above range. The resulting data are listed in Appendix A.3 and the algorithm is also described in detail in Appendix A.2. The results are shown in figure 4.3.

It can be found in figure 4.3 that, first, the points of the off Bragg angle blazing are continuous which means that for each value of h/λ we can find a definite d/λ correspondingly to obtain perfect blazing, and vice versa, and all these points makes a continuous curve which meets the curve for the Bragg blazing at about $h/\lambda=0.232, d/\lambda=0.902$. From the data behind, when the deviation becomes larger off Bragg blazing diverges further from the curve of Bragg blazing.

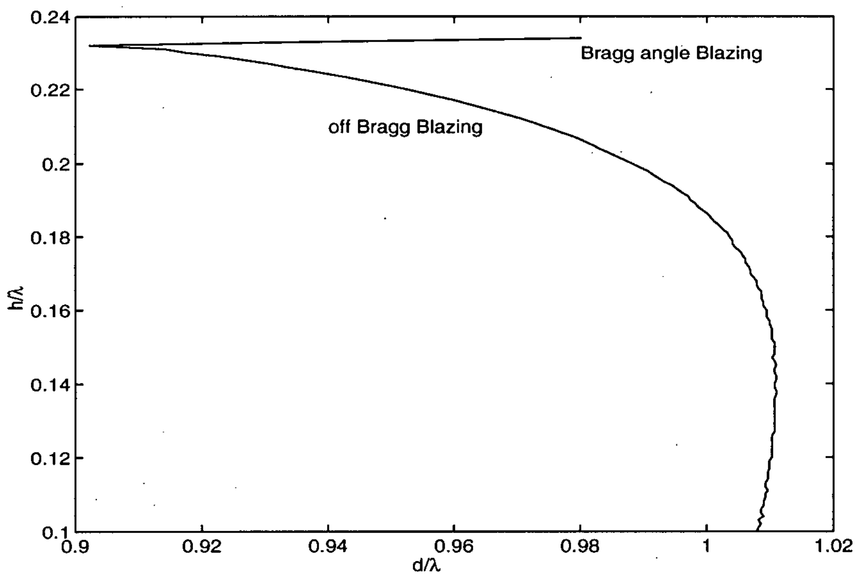

Figure 4.3 Design curve of off Bragg blazing with symmetrical rectangular gratings (a/d=0.5)

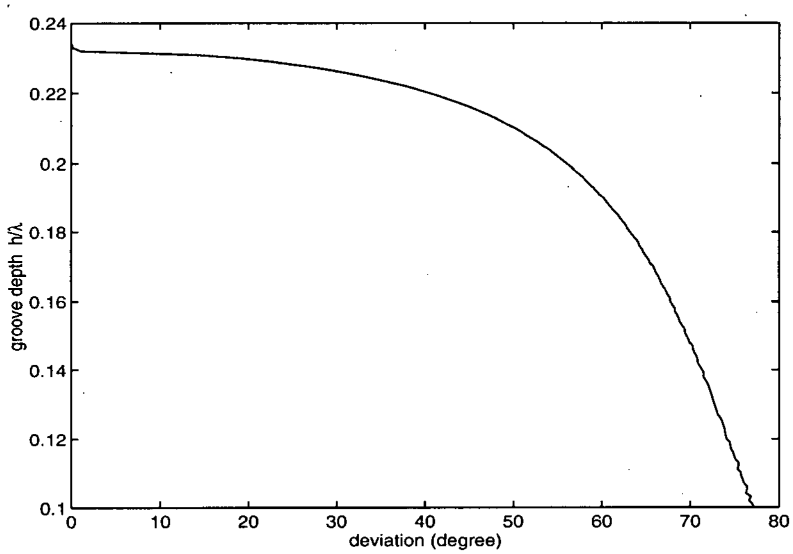

Figure 4.4 Groove depth vs. deviation for off Bragg blazing (a/d=0.5)

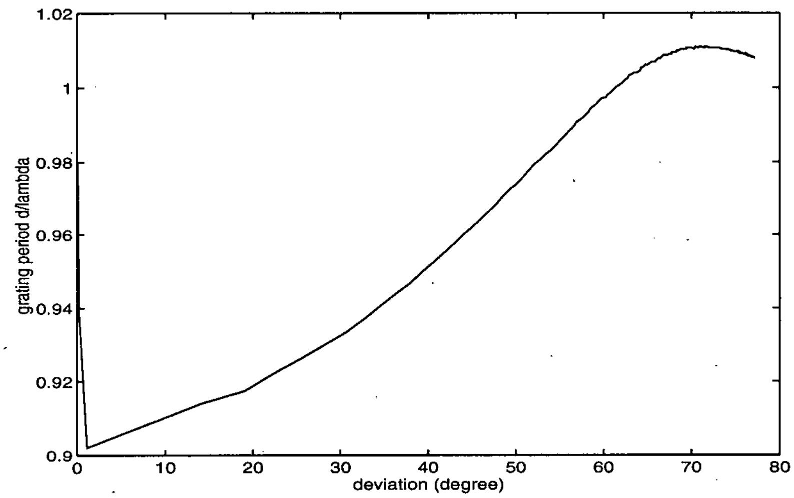

Figure 4.5 Grating period vs. deviation for off Bragg blazing

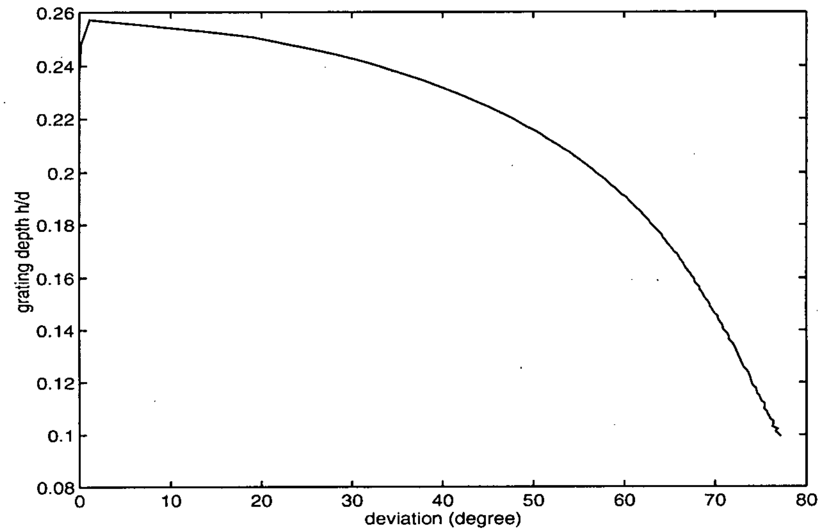

Figure 4.6 Grating depth h/d vs. the deviation for off Bragg blazing (a/d=0.5)

The curve of groove depth (h) vs. deviation is shown in figure 4.4, in which we can see that the larger the deviation the smaller the value of the h/λ should be to obtain off Bragg blazing.

Figure 4.5 shows the curve of period d/λ vs. the deviation. From figure 4.5 we find that for larger deviations we should chose larger values of the period d/λ to obtain off Bragg blazing.

From both figure 4.4 and figure 4.5, the tendency of the change of the blazing depth (h/d) vs. the deviation which is shown in the figure 4.6 can be predicted. When the deviation increases the blazing depth decreases.

If we exchange the x and y axes in figure 4.6, we get figure 4.7 which agrees almost exactly with results published by M.Breidne et al in [21] . Although the method used in [21] was an Integral Equation method, the results are same. This is a strong support for the accuracy of all our results.

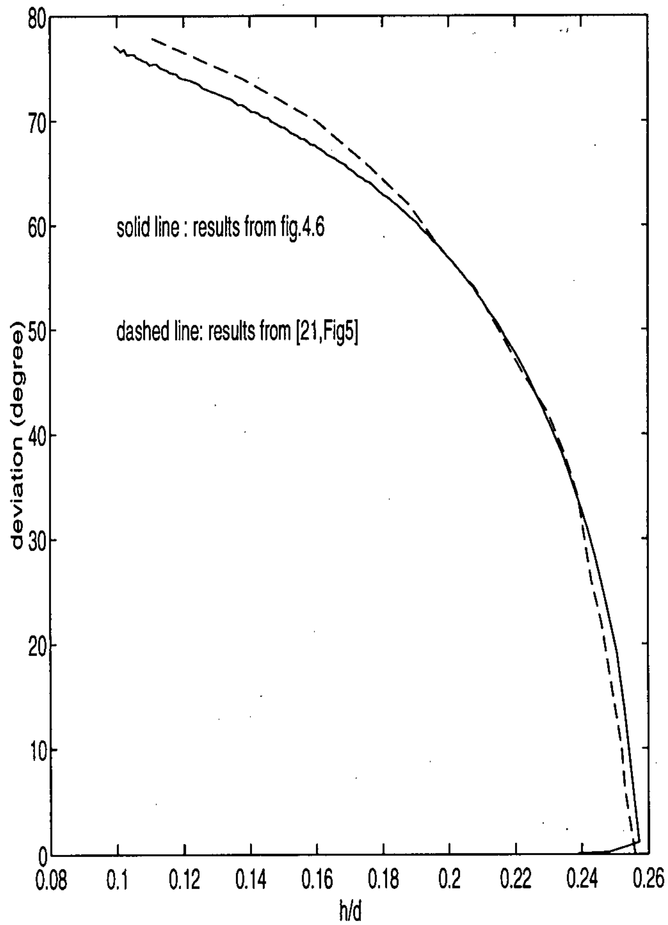

Figure 4.7 Comparison of results of fig.4.6 with results reported by Breidne [21, fig5].

Now, the question may be asked why we don't continue our search for h/λ<0.1. Since larger deviation may occur, the answer is that higher diffracted orders appear. As we shown before, off Bragg angle blazing angle will occur in pairs with two incidence angles θ_i^1andθ_i^2 . Taking into account the reciprocity theorem, the deviation (4.1) can also be written as:

$$D = \left|\theta_i^1 - \theta_i^2\right| \tag{4.3}$$

From the figure 4.3, we find that the further the curve leaves the Bragg angle blazing curve, the larger the value of the deviation. So, when we continue to decrease the value of the groove depth h/λ, we encounter large values of deviation which means that, considering equation 4.3, we can cope with a situation in which the incident electromagnetic field illuminates the grating with a very large angle of incidence. Unfortunately, the required value of d/λ is larger than 1.0 for large values of incident angle. Taking into account figure 1.1,–2 or +1 orders of diffraction may appear in addition to 0,-1 orders. We have restricted our discussion to the case that only two diffraction modes (m=0, –1) are considered. So, in figure 4.3, and in the following discussion, we will not continue searching for very large values of deviation.

§4.3 Unsymmetrical Rectangular Gratings

§4.3.1 Off Bragg Blazing for Unsymmetrical Rectangular Gratings

As stated earlier, the report of off Bragg angle blazing with the sinusoidal gratings motivates us to develop a research topic — off Bragg angle blazing with the rectangular gratings. Because only between the sinusoidal and symmetrical rectangular (a/d=0.5) gratings there exists the equivalence rule which will be described in Appendix A1, until now, all we discussed is TM polarization with the symmetrical rectangular gratings. Now that we have obtained some interesting results for the symmetrical rectangular gratings, naturally, we extend our investigation to the ordinary rectangular gratings whose a/d is not equal to 0.5.

Similarly, we consider the periodicity of the rectangular gratings first. But, unfortunately, the interesting periodicity that occurs for the symmetrical rectangular gratings does not appear for the unsymmetrical ones. However, keeping other parameters unchanged, there does exist more than one value of h at which the off Bragg angle blazing occurs.

Choosing a/d=0.6, 2/3, 0.7, 0.75 as examples, after the same exhaustive search as in the last section, it is interesting to find that off Bragg blazing for those four grating ratios (a/d) occur within a quite narrow range of h/λ.

Now, we adopt the same accurate searching algorithm as in the last section, and the design curves of groove depth (h/λ) vs groove period (d/λ) are shown in the figure 4.8.

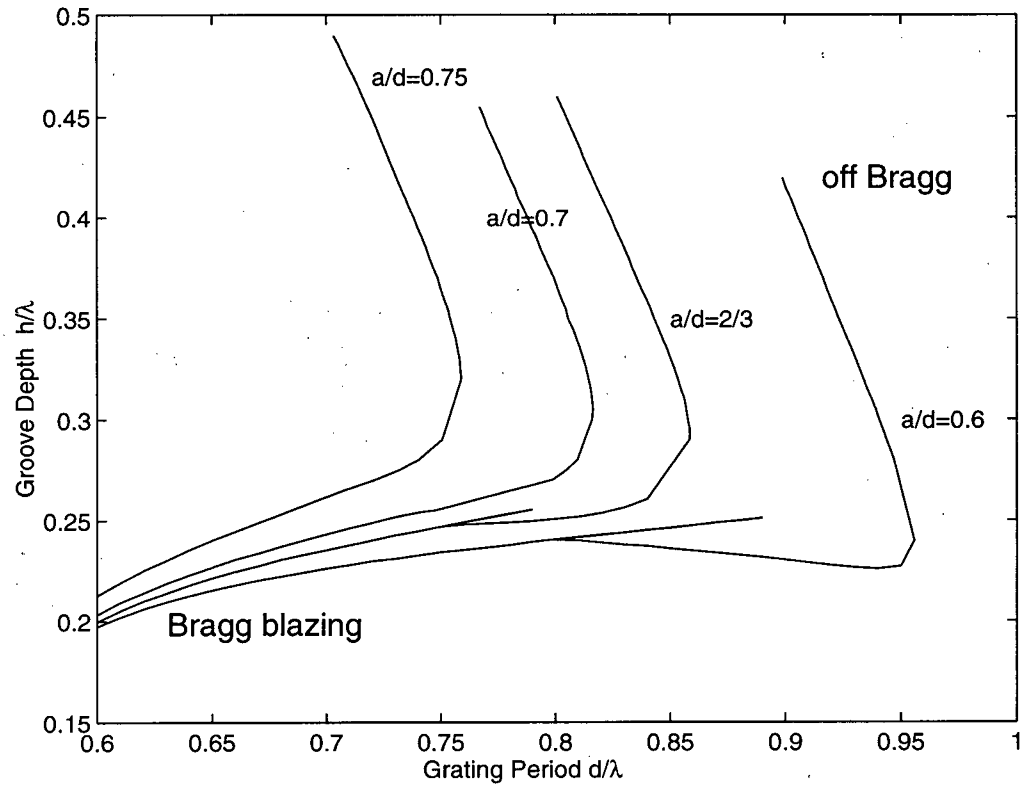

Figure 4.8 Design curves of off Bragg blazing for TM polarization with unsymmetrical rectangular gratings

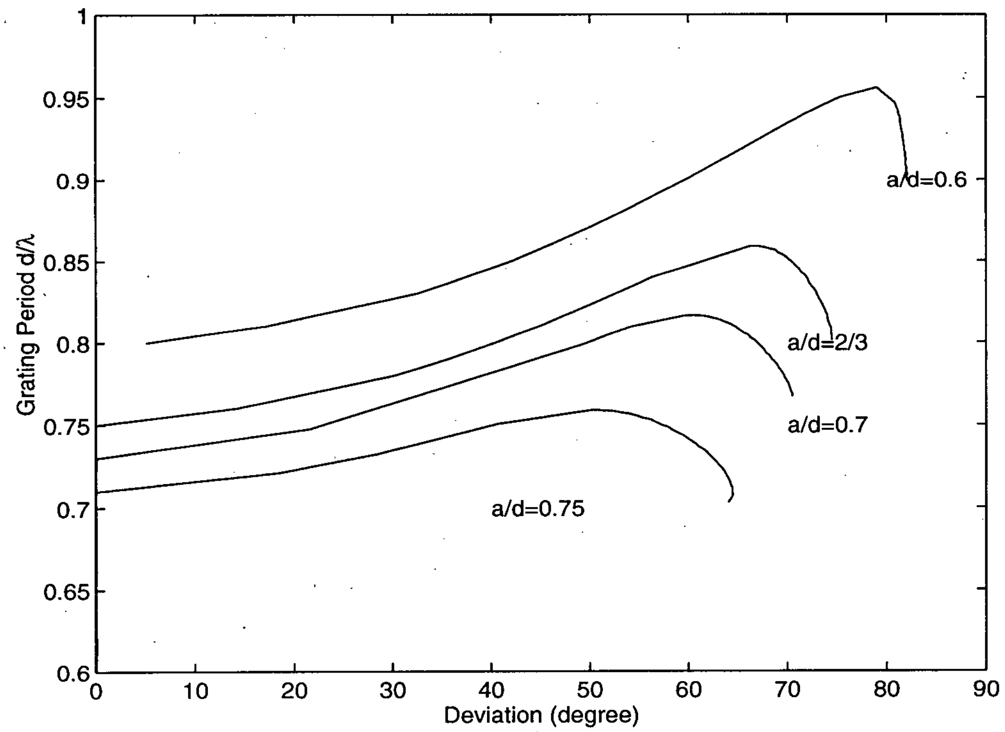

Figure 4.9 Off Bragg blazing as a function of the grating period vs. the deviation (when D=0, Bragg blazing occurs)

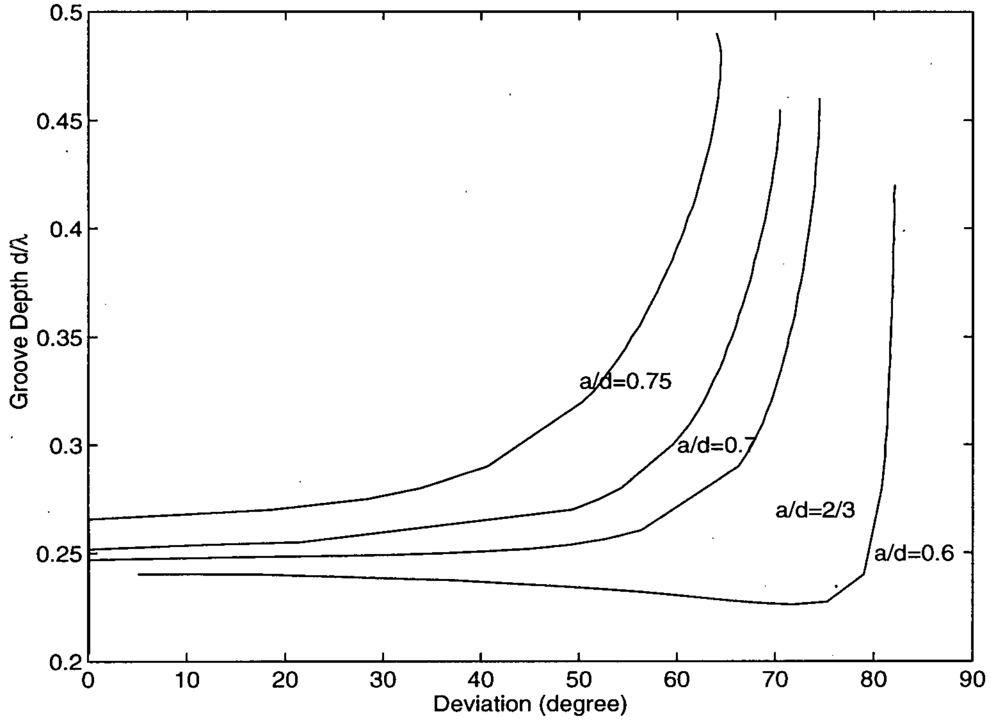

Figure 4.10 Off Bragg blazing as a function of groove depth vs. deviation

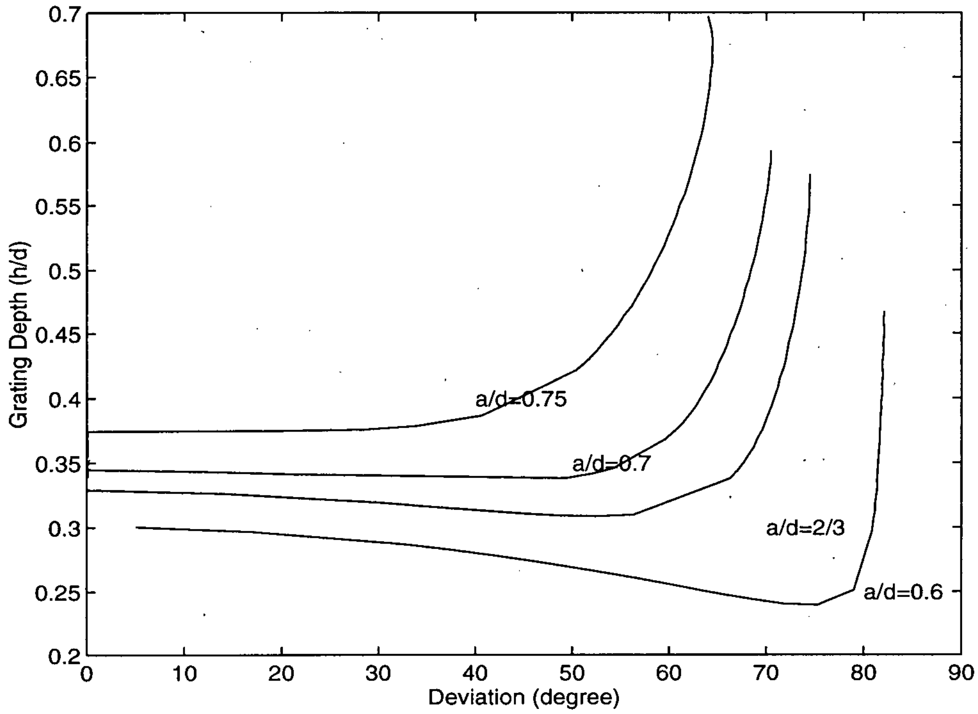

Figure 4.11 Off Bragg blazing as a function of the grating depth vs. deviation

All these curves begin from the curve for the Bragg angle blazing where the deviation is zero. In Figure 4.8 the further off the Bragg angle blazing curve, the larger the deviation is , which is similar to the behavior of the symmetrical rectangular gratings obtained in the last section. However, for the symmetrical rectangular gratings, when the deviation increases, the curve leaves the Bragg blazing curve and goes downwards, In contrast, here all these curves go upwards when the deviation increases.

Curves of the period d/λ vs the deviation are shown in figure 4.9. Figure 4.10 and 4.11 represent the groove depth (h/λ) and the relative grating depth (h/d) vs the deviation respectively. From those figures, we can find the property of the beginning points of these curves as that when the grating ratio (a/d) increases, the beginning point has a larger value of groove depth (h/λ) but a smaller value of period (d/λ).

There is apparently a continuity between the curves as the aspect ratio (a/d) varies, which makes figure 4.8 useful to predict the position of the similar curves for other values of a/d.

Because of the parity property of angles for off—Bragg blazing, and considering equation (4.3), off—Bragg blazing will disappear when the deviation is too large. So, all the curves of Figures 4.8–4.11 are continuous in a definite region and stop at a larger value of the deviation. In comparison, Bragg blazing is continuous in the whole region.

§4.3.2 Further Discussion

There also remains some interesting phenomena, details of which are discussed in this section. As seen in Figure 4.8 all the curves go upwards when the deviation increases. On the other hand the curve of off Bragg blazing for symmetrical rectangular (a/d=0.5) goes downwards.

From figure 4.12, we can discover when this change occurs. In figure 4.12 two curves (a/d=0.58, a/d=0.56) go upwards while another two curves go downwards (a/d=0.54, a/d=0.52). So, we can predict that the change occurs at about a/d=0.55.

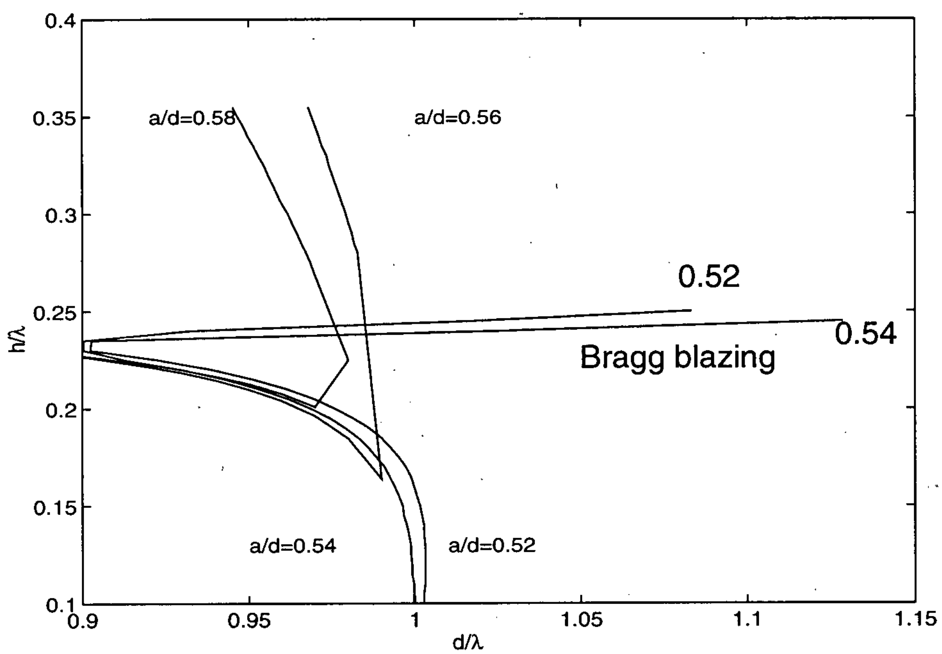

Figure 4.12 Bragg and Off Bragg Design Curves
for a/d=0.52,0.54,0.56,0.58

Another phenomena which should be discussed here is that from both figure 4.11 and figure 4.12, curves for a/d=0.6,0.58,0.56 go downwards first then go upwards. Thus all these curves have a singular point. Furthermore, the curves form an angle at this point, and when the a/d decreases, the degree of the angle decreases also.

Because the curve goes downwards then upwards, the curve of off Bragg blazing will cross the curve of Bragg blazing at a certain point. This interesting phenomena will be discussed next.

Now we choose a/d=0.56 as an example which is replotted in figure 4.13. We find that the cross over point occurs at about d/λ=0.98,h/λ=0.25. After calculations in the area around this point, we plot our results in figures 4.14 and 4.15.

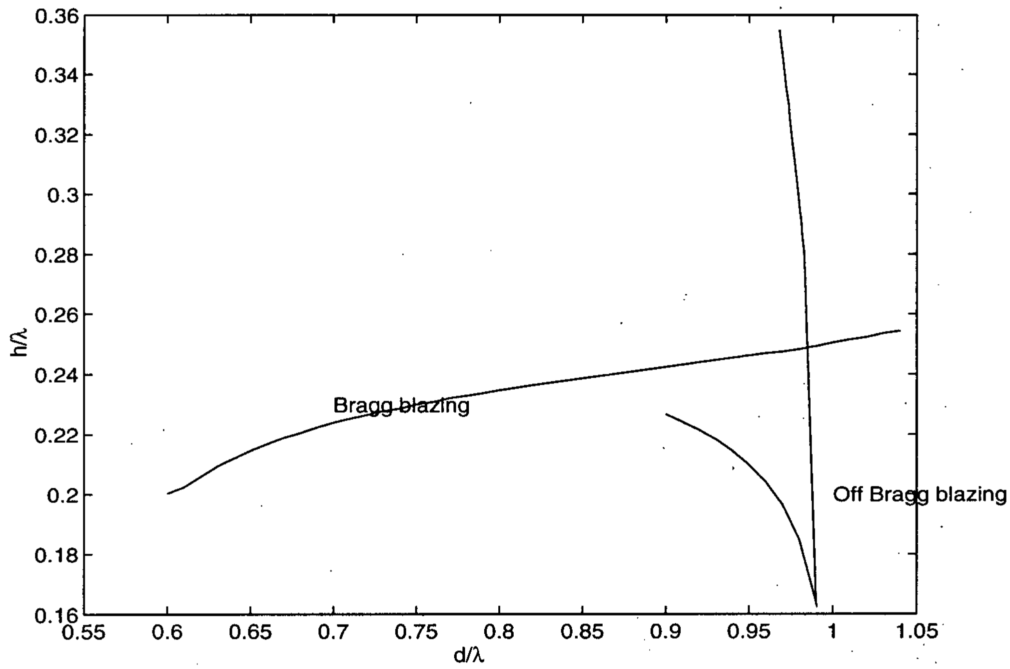

Figure 4.13 Bragg and Off Bragg blazing curves for a/d=0.56

Figure 4.14 shows the trend of the change for values of h/λ just below the cross over value. Choosing h/λ=0.2, d/λ=0.98, we find off Bragg blazing . Increasing h/λ to about 0.21, we find that off Bragg blazing has decreased; Continue increasing the depth of groove until h/λ=0.24, we find that off Bragg blazing has almost disappeared, and instead, we find Bragg blazing .

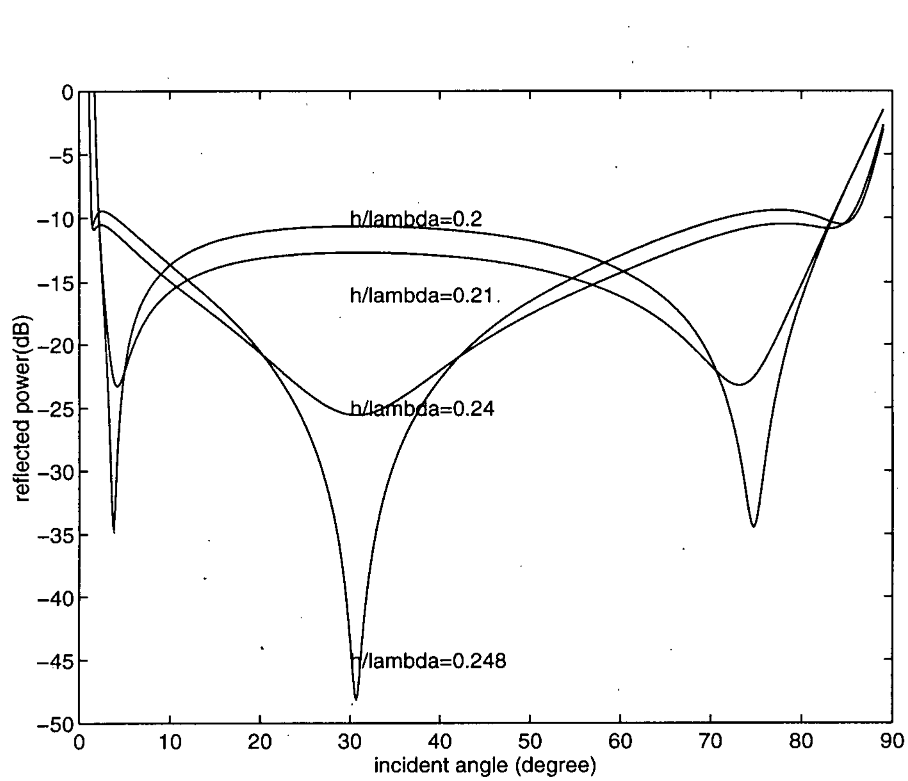

Figure 4.14 Reflected power vs. angle of incidence for various groove depth with a/d=0.56, d/λ=0.98

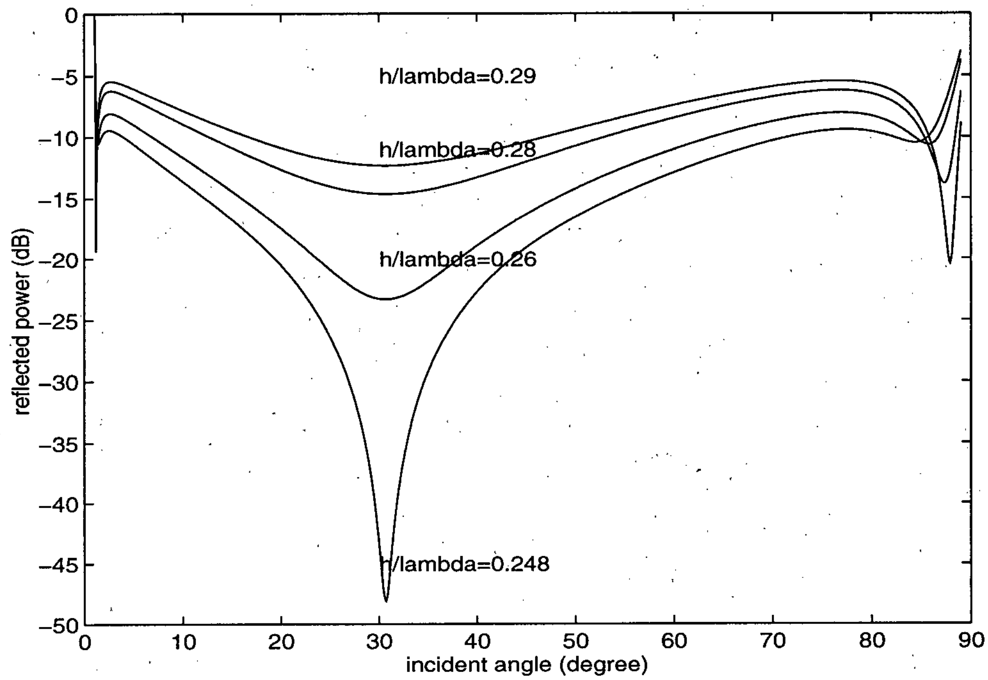

Figure 4.15 Reflected power vs. angle of incidence for various groove depth a/d=0.56, d/λ=0.98

Similarly, figure 4.15 shows the trend of the change for h/λ just above the cross over value. Starting from the cross over point, while h/λ increases, the Bragg blazing phenomena decreases until h/λ=0.28 where off Bragg blazing appears.

From figures 4.13, 4.14 and 4.15, we find that near the cross over point, there exists a quite large region (in our example, h/λ from 0.21 to 0.28) where it is quite difficult to distinguish between these two kinds of blazing. In this region, there is a change from one blazing to the other, and this indicates the relationship between these two kinds of blazing.

The changing from one blazing to the other was first reported earlier [12] from numerical results. The difference is that frequency and groove width were used as a variable parameters, while we change the depth of groove. However, the results are quite similar.

The third problem we will discuss in this section is off Bragg blazing for comb gratings. From figure 4.8, it can be seen that when a/d increases, off Bragg blazing may occur for deeper groove gratings. We use the mode match method here which allows us to check deep groove gratings. Results are shown in figure 4.16. In figure 4.16, we checked a/d=0.8,0.9 and 0.9999, and found off Bragg blazing there. If we approximate a/d=0.9999 to a comb grating, we can get the result that off Bragg blazing also occurs for comb gratings which was first observed in unpublished results by N.C. Beaulieu, E.V.Jull in 1981. Only an isolated example was given at that time, while here we provide the design curves.

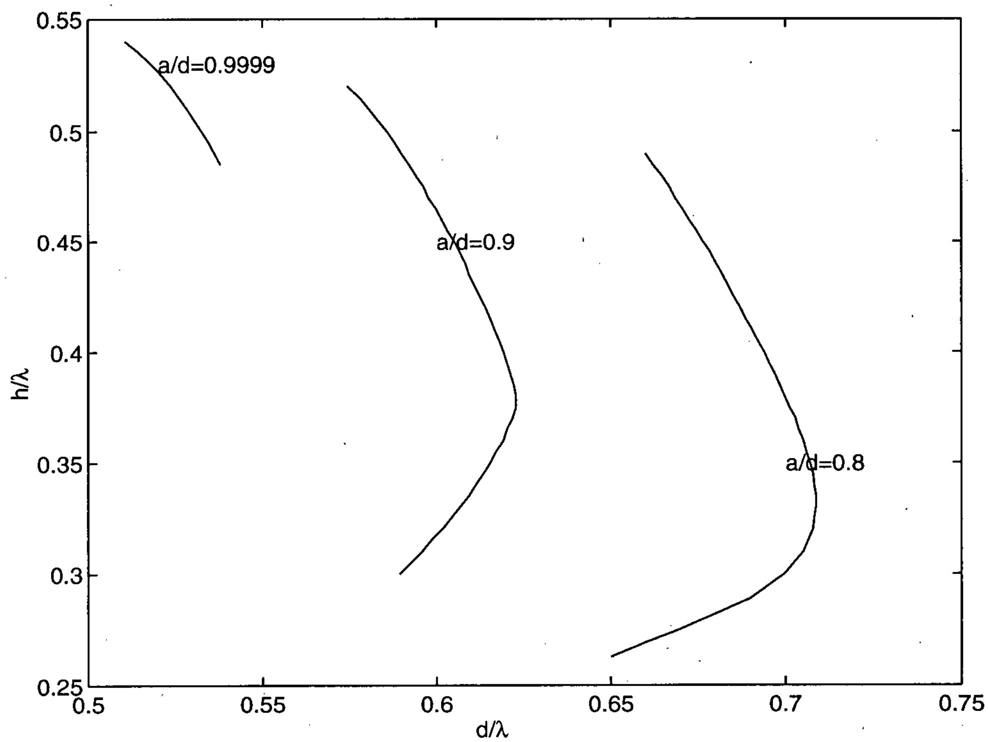

Figure 4.16 Design Curves for a/d=0.8,0.9,0.9999

Finally, we should discuss off Bragg blazing for narrow grooves. Until now, all gratings we checked have a/d greater than or equal to 0.5. So, it's quite natural to check gratings with a/d less than 0.5. However, unfortunately during the research of this thesis we didn't find off Bragg blazing occurring for the gratings with a/d much less than 0.5. From figure 4.8, 4.12 we can predict that when the value of a/d decreases, design curves shift right. From figure 4.3 when a/d is equal to 0.5, part of design curve enter the region where d/λ bigger than 1.0. So, if we choose a/d much less than 0.5, design curves may be plotted in the region where d/λ bigger than 1.0, then unfortunately from figure 1.1, m=+1 or m=-2 mode will appear, and high efficiency diffract gratings are not obtained.

Chap 5. Verification, Conclusions and Recommendation

Nothing provides more powerful evidence to verify the numerical results than experimental measurements. For this, we rely on previous measurements. After checking earlier experimental data, it is very interesting to find that a set of experimental data which was expected to be used to verify the result of the Bragg blazing [10] did display the particular property of off Bragg blazing. Using our program with the dimensions of the experimental grating, we find our result for off Bragg blazing is closer to the measurements than the previous numerical result for Bragg blazing. This is shown in the figure 5.1.

According to the dimensions of the experimental plate, $a/d=0.39, d/\lambda=1.46$, $h/\lambda=0.65$, and from figure 1.1 we can predict that off Bragg blazing may occur in a very narrow region around 20 degrees, which was shown exactly in figure 5.1. The two singular points in figure5.1 are Wood's anomalies [1].

As indicated in the first chapter, the aim of this study is to check the existence of off Bragg angle blazing and try to find some properties for such blazing with rectangular gratings. At the end of this thesis, a review of all results displayed before allows the following conclusions to be drawn.

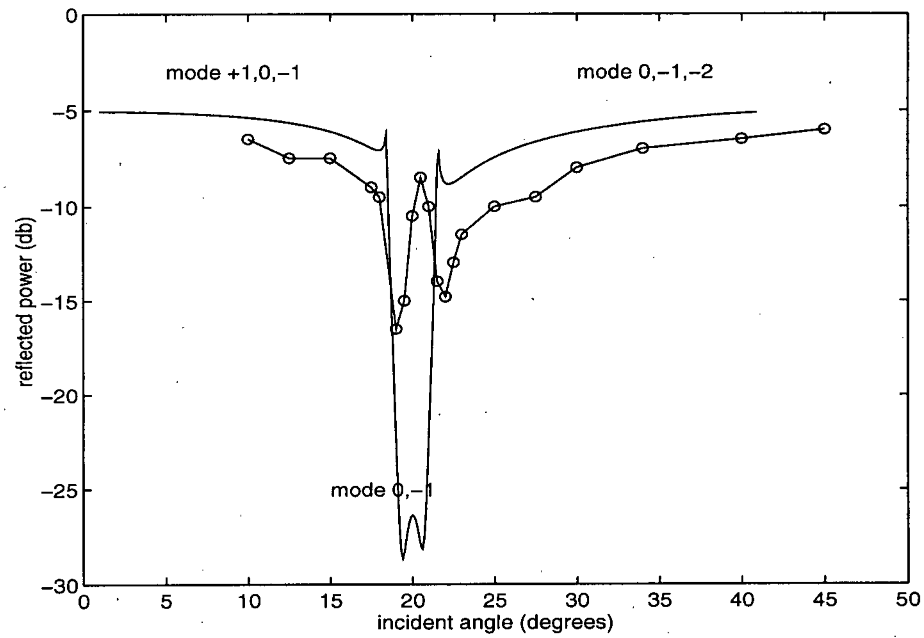

Figure 5.1 Measured and Calculated Reflected Power vs. incident angle (experimental data is from [10] : d=12.54mm,a=4.9mm,h=5,58mm f=35.0Ghz)
experimental data: ⊖—⊖—○
calculated data: ————

(1) Following the similar procedures proposed by Maystre et al [19] to find out off Bragg blazing with the sinusoidal gratings, by using the scattering matrix technique and the mode matching method, we first theoretically show the existence of the off Bragg blazing with rectangular gratings.

(2) Using the reciprocity theorem, we first define the range of the incident angle for off Bragg blazing, and find that when only two scattering orders exist, off Bragg blazing angles should occur in pairs. Furthermore, we give the basic

equation between these two incident angles.

(3)Using the mode matching method and a numerical search technique we first report design curves for off Bragg angle blazing in the last chapter, from which we find some interesting properties for such perfect blazing for TM polarization with the rectangular gratings.

First, we find that for symmetrical rectangular (a/d=0.5) gratings, there exists a periodicity which is very similar to the situation for Littrow mounting. Although such periodicity is not found for the unsymmetrical rectangular gratings, if we keep other variables (a,d,λ and deviation) unchanged, there exists more than one value of the groove depth h at which off Bragg angle blazing occurs

Then, we find that all design curves start from the Bragg angle blazing for which deviation equals to zero. When the deviation increases, the curve for off Bragg blazing leaves the curve for Bragg blazing. All these curves end with very large value of deviation at which the off Bragg blazing disappears. Compared with the continuity of the Bragg blazing in the whole range of dimensions, off Bragg blazing may be continuous only within some finite range.

Finally, by using these design curves, perfect blazing for other dimensions can be predicted. Moreover, taking into account equivalence rules, similar properties may be also found in other commercial gratings such as sinusoidal and echelette gratings.

All our results are for the TM polarization. However, if we review the chapter 3, it can be seen that we did not restrict our derivation to TM polarization only, which means that there is a possibility that off Bragg blazing exists for TE polarization. This should be investigated.

From the last chapter, we can see that if we carefully choose the parameters a/d, d/λ, h/λ and deviation, we can obtain off Bragg blazing. Not all the relationships among them have been discovered in this thesis. To find these relationships, to give reasonable explanations, and to derive analytic equations for them may be another direction of future work.

REFERENCES

1. R.Petit, “Electromagnetic Theory of Gratings”, Springer–Verlag Berlin Heidelberg New York, 1980

2. R.Mittra, S.W.Lee, “Analytical Techniques in the Theory of Guided Waves ”, Macmillan, New York, 1971

3. J.W.Dettman,”Mathematical Methods in Physics and Engineering”, McGraw–Hill, 1969

4. R.Courant,D.Hilbert,"Methods of Mathematical Physics”, Interscience Publishers Inc., New York, 1953

5. M.C.Hutley, “Diffraction Gratings”, Academic Press Inc. (London), 1982

6. C.H.Wilcox, “Scattering Theory for Diffraction Gratings”, Springer–Verlag New York Berlin Heidelberg Tokyo, 1982

7. D.Maystre, “Diffraction Gratings”, SPIE Optical Engineering Press, 1992

8. D.G.Michelson,“Radar Cross Section Enhancement for Radar Navigation and Remote Sensing”, 1993 UBC Dept. of Electrical Engineering PhD Thesis

9. H.William, “Numerical Receipes in Fortran” 2nd ed., Cambridge, New York, 1992

10. J.W. Heath, “Scattering by a Conducting Periodic Surface with

a Rectangular Groove Profile", June, 1977 UBC Dept. of Electrical Engineering M.A.Sc. Thesis

11. E.V.Jull and J.W.Heath,"Radio applications of rectangular groove corrugations", 1979 IEEE Antennas and Propagation International Symp., pp.515–518

12. E.V.Jull and N.C.Beaulieu, "An unusual grating behavior suitable for efficient frequency scanning",1980 IEEE Antennas and Propagation International Symp. pp.189–191

13. N.C. Beaulieu, "TM Blazing of Rectangular Groove Gratings off the Bragg Angle", Dec. 1979. UBC Dept. of Electrical Engineering. Elec 498 Project Report.

14. A.Hessel, J.Shmoys and D.Y.Tseng,"Bragg-angle Blazing of Diffraction Gratings"J.Opt.Soc.Am., Vol65 No.4, pp.380–384, Apr. 1975

15. E.V.Jull, J.W.Heath and G.R.Ebbeson,"Gratings that Diffract All Incident Energy", J.Opt.Soc.Am., Vol67,No.4,pp.557–560, Apr 1977

16. E.V.Jull, G.R.Ebbeson, "The Reduction of Interference from Large Reflecting Surfaces", IEEE Trans. AP.,pp. 565–570, July 1977.

17. J.W.Heath, E.V.Jull, "Perfectly Blazed Reflection Gratings with Rectangular Grooves", J.Opt.Soc.Am. Vol 68, No.9, pp.1211–1216, Sept. 1978.

18. M.Breidne, D. Maystre, "Equivalence of Ruled, Holographic and Lammellar Gratings in Constant Deviation Mountings ", Applied Optics, Vol.19, No.11, pp.1812–1820, June 1980

19. D.Maystre, M.Cadilhac, "Gratings: a phenomenological approach and its applications, perfect blazing in a non-zero deviation mounting", Optica, Acta. 1981, Vol28, No.4, pp.457–470

20. Wei Chen, N.C.Beaulieu, D.G.Michelson, E.V.Jull, "TM Blazing of Rectangular Groove Gratings at Non-Bragg Incidence", IEEE AP-S Symp, June, 1994

21. M Breidne, D.Maystre, "Perfect blaze in non-Littrow mountings", Optic Acta, 1981, vol.28,no10, 1321–1327

22. A. Wirgin, "On the Theory of Scattering from Rough Lamellar Surfaces", Alta Freq. , vol. 38, pp. 327–331, 1969

Appendix A.1 Equivalence Rules

Maystre et al [18] in 1980 first proposed the equivalence of symmetrical triangular, sinusoidal and symmetrically rectangular gratings. For equivalence these three different grating profiles have almost the same efficiency curves. However, the equivalence rule is applicable in the case of the following two conditions being satisfied. First, only two orders propagate — specular reflection (m=0) and principal backscattering(m=-1); Second, the gratings must have a profile with a centre of symmetry i.e. only gratings having a profile that can be expanded in a Fourier sine series satisfy the equivalence rule.

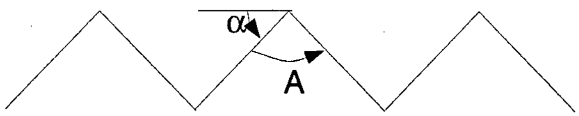

(a)

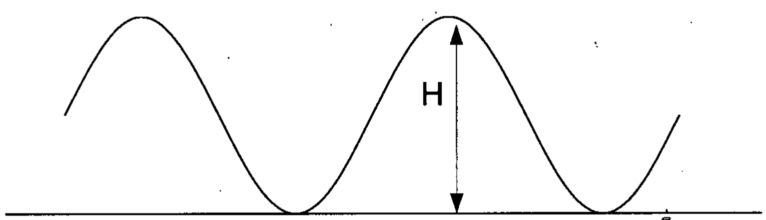

(b)

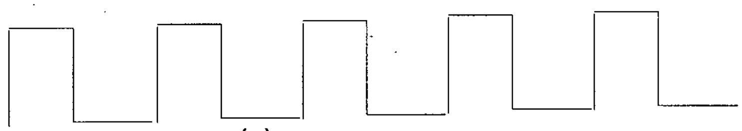

Figure A.1 Equivalent grating profiles

Figure A.1 (a) (b) (c) display three kinds of gratings that can be expanded in a sine series:

$$f(x) = \sum_{n=1}^{\infty} b_n \sin Kx \qquad \text{(A.1)}$$
$$K = 2\pi/d$$

For the ruled grating with triangular profile in figure A.1(a):

$$b_n = \frac{d}{(n\pi)^2}[\tan\alpha - \tan(A+\alpha)].\sin\left[\frac{\pi n \sin(A+\alpha)\cos\alpha}{\sin A}\right] \qquad \text{(A.2)}$$

Similarly equation (A.3)(A.4) represent the b for the sinusoidal and symmetrical rectangular gratings respectively:

$$b_1 = H/2, \qquad b_n = 0, n = 1, 2, ... \qquad \text{(A.3)}$$

$$b_n = \frac{2H}{n\pi} \qquad n = 1,3,5,..; b_n = 0 \qquad n = 2,4,6,.. \qquad \text{(A.4)}$$

When only two diffraction orders are considered, it can be shown that even the first harmonic in the Fourier series above has little influence on the efficiency. The proof is given below:

Assuming a profile given only by the fundamental and the first harmonic of a Fourier sine series:

$$y = f(x) = b_1 \sin Kx + b_2 \sin 2Kx \tag{A.5}$$

Keeping other parameters unchanged, the efficiency of the ith order of diffraction is a function of b1 and b2 such as $E_i(b_1, b_2)$. The efficiency is unchanged by a translation along the x axis. In particular for a translation d/2, we get

$$E_i(-b_1, b_2) = E_i(b_1, b_2) \tag{A.6}$$

Taking into account reciprocity for grating having the profile given by y=f(-x), we can get:

$$E_i(-b_1, -b_2) = E_i(b_1, b_2) \tag{A.7}$$

Because only two orders of diffraction propagate, so:

$$E_0(b_1, b_2) + E_{-1}(b_1, b_2) = 1 \tag{A.8}$$

From (A.6),(A.7),(A.8), we get:

$$E_i(b_1, b_2) = E_i(-b_1, b_2) = E_i(b_1, -b_2) = E_i(-b_1, -b_2), i = 0, -1 \tag{A.9}$$

Considering the development of $E_{-1}(b_1, b_2)$in a Taylor series. Equation A.8 makes the series have only even terms:

$$E_{-1}(b_1, b_2) = \alpha_0 + \alpha_1 b_1^2 + \alpha_2 b_2^2 + \alpha_3 b_1^4 + \alpha_4 b_2^4 + .. \tag{A.10}$$

For the gratings in figure A.1 $b_2^2 << b_1^2$, so that the amplitude of the first harmonic has much less influence on the efficiency than the amplitude of the fundamental.

If only the fundamental term is considered only, from equation A.2 and A.3, the symmetrical rectangular grating whose depth is $\pi/4$ times that of the associated sinusoidal grating may has almost the same efficiency curve as that of the associated sinusoidal grating. Other equivalence rules are described in detail in [18].

Appendix A.2 Golden Section Search

A minimum is known to be bracketed between a and c only when there is a triplet of points, a<b<c such that f(b) is less than both f(a) and f(c). In this case we know that the function has a minimum in the interval (a,c).

The algorithm of minimum search is to choose a new point of x either between a and b or between b and c. Suppose here we make the latter choice. Then if f(b)<f(x) then the new bracketing triplet is (a,b,x), otherwise, it is (b,x,c). We continue the process until the distance between the two outer points of the triplet is tolerably small.

Now the problem is that how to choose the position of the new point of x. Assuming a,b,c satisfy equation A.11:

$$\frac{b-a}{c-a} = w, \qquad \frac{c-b}{c-a} = 1-w \tag{A.11}$$

and assuming that the new point x satisfies equation A.12:

$$\frac{x-b}{c-a} = z \tag{A.12}$$

Then, the next bracketing segment will wither be w+z or 1–w, to minimize the worst case possibility, we should choose z to make them equal

$$z = 1 - 2w \tag{A.13}$$

Furthermore, if z is chosen to be optimal, then so was w before it, which implies that x should be the same fraction of the way from b to c as was b from a to c or:

$$\frac{z}{1-w} = w \tag{A.14}$$

Solving equations A.13, A.14, we get w=0.38197 which is called the golden mean or golden section.

Appendix A.3 Data List

The following is a collection of data, most of which appears in graphical form in Chapter 3 and Chapter 4

Table 1. TM polarization for a/d=0.5

Depth (h/λ)	Period(d/λ)	Reflection Efficiency(db)	Deviation (degree)
0.10	1.00	-44.39	77.20
0.11	1.01	-47.28	75.69
0.12	1.01	-47.59	74.14
0.13	1.01	-52.16	72.77
0.14	1.01	-51.05	71.36
0.15	1.01	-50.97	69.41
0.16	1.00	-51.94	67.72
0.17	1.01	-57.45	65.45
0.18	1.00	-59.78	62.91
0.19	0.99	-62.09	59.74
0.20	0.99	-62.22	55.03
0.21	0.97	-83.45	48.57
0.22	0.95	-81.05	37.89
0.23	0.90	-95.25	1.12

Table 2. TM polarization for a/d=0.6

Depth (h/λ)	Period (d/λ)	Reflection Efficiency (db)	Deviation (degree)
0.20	0.60	-64.75	0.08
0.22	0.65	-66.38	0.03
0.23	0.70	-60.13	0.03
0.23	0.75	-63.47	0.02
0.24	0.82	-61.61	0.06
0.25	0.87	-60.90	0.04
0.24	0.83	-62.60	32.54
0.23	0.88	-66.10	53.38
0.23	0.93	-63.96	68.72
0.29	0.94	-48.58	80.93
0.31	0.94	-49.21	81.38
0.35	0.92	-39.96	81.72
0.38	0.91	-47.75	81.87
0.40	0.91	-36.65	81.98

Table 3. TM polarization for a/d=0.7

Depth (h/λ)	Period (d/λ)	Reflection Efficiency (db)	Deviation (degree)
0.20	0.60	-59.06	0.08
0.22	0.63	-66.72	0.05
0.23	0.66	-62.29	0.10
0.24	0.69	-69.66	0.08
0.25	0.72	-58.24	0.03
0.26	0.75	-82.67	21.57
0.28	0.81	-65.91	54.30
0.31	0.82	-60.29	61.33
0.33	0.81	-58.86	63.21
0.34	0.81	-50.76	64.76
0.36	0.80	-62.94	65.98
0.37	0.80	-47.83	67.01
0.39	0.79	-46.03	67.84
0.40	0.79	-55.41	68.73
0.42	0.78	-44.34	69.40
0.43	0.78	-40.38	69.90
0.45	0.77	-32.25	70.32

Table 4. TM polarization for a/d=0.8

Depth (h/λ)	Period (d/λ)	Reflection Efficiency (db)	Deviation (degree)
0.26	0.65	-65.13	0.03
0.28	0.68	-68.97	0.06
0.30	0.71	-87.08	0.05
0.32	0.71	-65.35	34.06
0.34	0.71	-59.33	39.20
0.35	0.71	-75.47	42.92
0.37	0.70	-52.20	45.96
0.38	0.70	-51.09	48.56
0.40	0.69	-51.52	50.85
0.41	0.69	-53.78	52.75
0.43	0.69	-42.93	54.37
0.44	0.68	-48.19	55.81
0.46	0.67	-43.56	56.78
0.47	0.67	-34.21	57.53
0.49	0.66	-28.41	57.89

Table 5. TM polarization for a/d=0.9

Depth (h/λ)	Period (d/λ)	Reflection Efficiency (db)	Deviation (degree)
0.30	0.59	-61.67	0.07
0.32	0.60	-56.43	0.03
0.33	0.61	-63.82	0.00
0.35	0.61	-59.39	0.01
0.36	0.62	-62.15	0.10
0.38	0.62	-57.51	4.67
0.39	0.62	-65.89	17.37
0.41	0.62	-71.62	24.60
0.42	0.61	-61.53	29.85
0.44	0.61	-45.45	34.12
0.45	0.60	-49.21	37.23
0.47	0.60	-52.13	39.78
0.48	0.59	-43.29	41.62
0.50	0.59	-42.68	42.62
0.51	0.58	-31.30	42.64

Table 6. TM polarization for a/d=0.9999

Depth (h/λ)	Period (d/λ)	Reflection Efficiency (db)	Deviation (degree)
0.48 5	0.54	-69.53	3.92
0.49 0	0.54	-59.43	9.69
0.495	0.53	-66.66	12.73
0.500	0.53	-51.06	15.05
0.505	0.53	-48.20	16.63
0.510	0.53	-48.84	17.80
0.515	0.53	-45.92	18.62
0.520	0.52	-56.55	19.07
0.525	0.52	-53.46	19.08
0.530	0.52	-44.52	18.59
0.535	0.51	-37.00	17.63
0.540	0.51	-30.95	15.57

Table 7. TM polarization for a/d=0.4

Depth (h/λ)	Period (d/λ)	Reflection Efficiency (db)	Deviation (degree)
0.150	1.02	-55.50	81.59
0.155	1.03	-56.79	81.38
0.160	1.03	-62.37	81.07
0.165	1.03	-53.12	80.79
0.170	1.04	-56.55	80.63
0.175	1.04	-56.31	80.38
0.180	1.05	-63.09	80.20
0.185	1.05	-62.25	80.0347 79.92
0.190	1.06	-58.05	79.92
0.195	1.07	-58.67	81.18
0.210	1.12	-64.90	81.64
0.212	1.13	-55.37	82.52
0.215	1.15	-62.20	

Table 8. TM polarization for a/d=0.52

Depth (h/λ)	Period (d/λ)	Reflection Efficiency (db)	Deviation (degree)
0.10	1.00	-54.91	80.91
0.11	1.00	-51.44	79.66
0.12	1.00	-43.11	78.36
0.13	1.00	-47.49	76.93
0.14	1.00	-66.66	75.44
0.15	1.00	-53.16	73.89
0.16	1.00	-50.83	72.15
0.17	1.00	-55.31	70.08
0.18	1.00	-64.49	67.63
0.19	0.99	-61.62	64.53
0.20	0.98	-57.92	60.57
0.21	0.96	-65.46	54.86
0.22	0.94	-85.41	45.91
0.23	0.90	-77.75	27.57
0.24	1.03	-70.50	0.06

Table 9. TM polarization for a/d=0.54

Depth (h/λ)	Period (d/λ)	Reflection Efficiency (db)	Deviation (degree)
0.10	1.00	-44.11	84.22
0.11	1.00	-40.12	82.89
0.12	1.00	-44.06	81.85
0.13	1.00	-44.08	80.46
0.14	1.00	-55.73	79.23
0.15	1.00	-48.45	77.62
0.16	0.99	-58.86	76.03
0.17	0.99	-53.72	74.02
0.18	0.99	-66.34	71.73
0.19	0.98	-70.20	68.88
0.20	0.97	-63.78	65.09
0.21	0.95	-60.59	59.59
0.22	0.93	-85.09	51.17
0.23	0.90	-43.85	36.33
0.24	0.93	-77.04	0.09

Table 10. TM polarization for a/d=0.56

Depth (h/λ)	Period (d/λ)	Reflection Efficiency (db)	Deviation (degree)
0.23	0.90	-69.23	47.92
0.22	0.92	-64.43	55.16
0.21	0.94	-62.67	61.79
0.20	0.96	-63.19	68.09
0.18	0.98	-68.44	75.09
0.28	0.98	-37.60	87.07
0.29	0.98	-39.88	86.97
0.30	0.98	-45.49	86.85
0.32	0.97	-34.59	86.71
0.33	0.97	-37.33	86.71
0.34	0.97	-34.92	86.57
0.35	0.97	-37.62	86.55

Table 11. TM polarization for a/d=0.58

Depth (h/λ)	Period (d/λ)	Reflection Efficiency (db)	Deviation (degree)
0.23	0.90	-71.15	54.46
0.22	0.92	-74.67	60.86
0.22	0.94	-62.84	66.96
0.21	0.96	-62.48	73.02
0.23	0.98	-63.64	84.26
0.27	0.97	-48.85	84.32
0.29	0.97	-44.43	84.26
0.30	0.96	-53.72	84.30
0.31	0.96	-40.33	84.22
0.32	0.96	-49.88	84.26
0.33	0.95	-43.70	84.30
0.34	0.95	-41.79	84.20

Table 12. TM polarization for a/d=2/3

Depth (h/λ)	Period (d/λ)	Reflection Efficiency (db)	Deviation (degree)
0.20	0.60	-60.11	0.11
0.22	0.64	-64.72	0.05
0.23	0.68	-62.86	0.06
0.24	0.72	-61.93	0.03
0.25	0.77	-69.34	0.02
0.25	0.78	-74.07	30.20
0.25	0.82	-59.60	48.89
0.30	0.86	-58.97	67.01
0.32	0.85	-49.85	69.08
0.34	0.85	-61.04	70.58
0.36	0.84	-52.46	71.71
0.38	0.83	-40.12	72.59
0.40	0.83	-46.46	73.27
0.42	0.82	-51.87	73.89
0.44	0.81	-43.74	74.26
0.46	0.80	-39.85	74.47

Table 13. TM polarization for a/d=0.75

Depth (h/λ)	Period (d/λ)	Reflection Efficiency (db)	Deviation (degree)
0.21	0.60	-56.12	0.08
0.24	0.64	-72.36	0.05
0.25	0.68	-65.09	0.06
0.27	0.72	-75.36	18.45
0.32	0.76	-66.18	50.36
0.34	0.76	-62.59	54.02
0.36	0.75	-51.53	56.73
0.38	0.75	-45.99	58.93
0.40	0.74	-57.01	60.75
0.44	0.72	-41.36	63.39
0.46	0.72	-46.25	64.17
0.48	0.71	-33.41	64.48